Effect of Elevated Temperature on Hydraulic Conductivity of Bentonite-Polymer Composite Geosynthetic clay liner to Saline Solutions

A Thesis submitted in partial fulfillment of the requirements for the degree of Master of Science at George Mason University

by

Andres Javier Cruz
Bachelor of Science
George Mason University, 2019

Director: Kuo Tian, Associate Professor
Department of Civil Engineering

Summer Semester 2021
George Mason University
Fairfax, VA

DEDICATION

This is dedicated to my supporting family, my dad Jorge, my mom Mirna, my brothers Alex and Carlos, and all of my friends who have helped me along this journey.

ACKNOWLEDGEMENTS

I would like to thank my family, professors, and friends who have helped me get this far. I would like to thank my parents who have had to listen to me during tough times and give me words of motivation and advice. My brothers who have always gave me words of advice as to how I should hold myself. I would like to thank Dr Tanyu for recruiting me for undergraduate research and expose me to the working culture of a researcher. I would like to thank Dr. Tian for coaching me through the entirety of my thesis research study. Thank you to all of my friends and coworkers who have been by my side through this entire research.

TABLE OF CONTENTS

LIST OF TABLES

LIST OF FIGURES

LIST OF ABBREVIATIONS

Bentonite Polymer Composite ..... BPC
Deionized water ..... DI water
Hydraulic Conductivity ..... HC
Geosynthetic Clay Liner ..... GCL
Municipal Solid waste ..... MSW
Pore Volume of Flow ..... PVF
Sodium Bentonite ..... NaB

ABSTRACT

EFFECT OF ELEVATED TEMPERATURE ON HYDRAULIC CONDUCTIVITY OF BENTONITE-POLYMER COMPOSITE GEOSYNTHETIC CLAY LINER TO SALINE SOLUTIONS

Andres Javier Cruz, M.S.

George Mason University, 2021

Thesis Director: Dr. Kuo Tian

Current regulation established for disposal of solid waste (e.g., municipal solid waste, and coal combustion residuals) requires disposal facilities to include a composite liner system consisting of a geomembrane overlying a 0.6-m-thick clay liner. Geosynthetic clay liners (GCLs) provide a sustainable alternative to use of in lieu of a conventional clay liner, due to benefits of GCLs having low hydraulic conductivity ($< 1 \times 10^{-10}$ m/s), thin to save air space, and easy to install. GCL consists of one layer of sodium bentonite sandwiched between two layers of geotextile that can be woven or non-woven. These GCLs can be modified through addition of polymerized bentonite, called bentonite polymer composite (BPC), to improve the chemical compatibility of GCLs against aggressive landfill leachates. Due to biodegradation of waste materials, each landfill has an associated temperature gradient that describes an increase in temperature with an increase in depth of the landfill causing leachate within to become hotter with depth of the

landfill (Yeşiller, N., and Hanson, J. L. 2003). So far, limited study has investigated the effect of elevated temperatures on the hydraulic conductivity of BPC GCLs

Four commercial GCLs were evaluated in this study, including three BPC GCLs and one Na-B GCLs. One BPC GCL consists of bentonite modified with cross-linked polymer and the other two BPC GCLs have liner polymer additives. Hydraulic conductivity tests were conducted with DI water, 20 mM $CaCl_2$ and 50 mM $CaCl_2$ solutions at temperatures of 20 ^oC, 35 ^oC, and 60 ^oC. Swell index tests (ASTM D5890) were conducted to analyze the swelling of BPC compared to Na-B at elevated temperatures. Viscosity tests were conducted to analyze rheology of BPC exposed to DI water, 20 mM $CaCl_2$ and 50 mM $CaCl_2$ solutions at elevated temperatures.

Both linear polymers produced an increase in hydraulic conductivity permeated with 50 mM $CaCl_2$ at elevated temperatures, however, BPC GCLs exposed to high temperatures show increase in swell index that can potentially affect hydraulic conductivity results. Additionally, viscosity of permeant solution decreases allowing more polymer to be flushed causing an increase in hydraulic conductivity. The cross link GCL showed little to no change in hydraulic conductivity with change in temperature, however, the elevated temperature test showed a reduction in overall polymer eluted. These observations indicated that the hydrogel swell allowed for less polymer to be eluted during permeation because of the larger size clogging polymer hydrogels between bentonite granules.

.

CHAPTER 1

Introduction

Geosynthetic clay liners (GCL) are commonly used as hydraulic barriers in containment infrastructure, such as municipal solid waste, mine tailings, and hazardous waste landfills (Rowe and Petrov 1997, Benson and Wang 1999 Shackelford 2000, Joe et al. 2001, Kolstad et al. 2004, Ishimori and Katsumi 2008, Tian et al. 2016; Touze-Foltz et al., 2018). GCL is a very thin material that are composed of a layer of sodium bentonite (NaB) sandwiched between two geotextile layers. Composite liner system used in landfill typically consists of a geomembrane layer overlain on a compaction clay liner or GCL. GCLs have been more accepted in the landfill barrier design due to low hydraulic conductivity, thin to save air space, and easy to installation. This GCL are normally 5 to 10 mm in thickness and provides low hydraulic performance to water (e.g., $<1 \times 10^{-10}$ m/s) (Shackelford et al. 2000, Joe et al. 2001, Kolstad et al. 2004, Ghandi et al 2016, Kartika et al 2013, Tian et al. 2016). The effectiveness of the conventional NaB GCL are primarily controlled by the swelling of montmorillonite soil within the GCL. Osmotic swelling of the montmorillonite allows GCL void spaces to close and result in a lower hydraulic conductivity. GCL permeated with solutions containing high ionic strength, predominant divalent cations, or extreme acidic or basic conditions will suppress osmotic swelling of

the bentonite, resulting in an increase in hydraulic conductivity (Shackelford et el. 2000, Jo et al. 2001, 2005, Kolstad et al. 2004, Tian et al. 2016, 2019).

Recognized these deficiencies, GCL has been modified through polymerization of molecules or addition of polymer hydrogel to improve its chemical compatibility to high strength leachates. GCLs are enhanced through polymerization or through dry addition of super absorbent polymers. NaB GCL modified by polymerized, or dry polymer mix, are considered bentonite-polymer composite, or BPC. BPC GCL's are able to maintain a hydraulic performance of $<10^{-10}$ (m/s) when exposed to solutions having a high ionic strength or pH condition (Kolstad et al. 2004, Katsumi et al. 2008, Scalia et al. 2014, Tian et al. 2016, 2019).

GCL that installed in the landfill liner system may experience elevated temperatures. For example, elevated temperature has been observed in MSW landfill due to the degradation of organic waste materials within the landfill (Mitchel 1993, Rowe 1998, Yesiller et al. 2005, Koerner and Koerner 2005). Yesiller et al. (2005) performed an in-depth analysis of the temperature gradients associated with depth of various municipal solid waste landfills at various locations. Temperature gradients were recorded and determined as the quotient of the temperature difference between two adjacent sensors within a vertical array of known distance between the sensors. The highest temperatures recorded at various MSW landfills was recorded as 57 ^{o}C with a temperature gradient ranging from as low as-30^{o} C/m to as high as +22^{o} C/m, with average gradient of 5^{o}C/m of depth. Rowe (1998) also recorded temperatures in excess of 60^{o}C within MSW landfill,

light industrial landfills, industrial solids and sludge landfill, and leachate recirculation landfills.

Bentonite swelling and permeant solution viscosity were variables that depend on temperature, which could affect the hydraulic barrier performance of GCL. Bentonite swelling are associated with the thickness of the diffuse double layer (DDL), that relates to the area of space where clay cations attach to water dipoles (Yeung 1992, Mitchell 1993, Shackelford 1994, Patel 2005). The DDL thickness (tdl) are as follows Eq. X. (Yeung 1992, Mitchell 1993)

$$t_{dl} = \sqrt{\frac{\varepsilon\varepsilon_0 RT}{2v^2F^2\eta}} \qquad \text{Equation 1.}$$

Where ε is the dielectric constant of the pore water, which are temperature dependent, ε_0 is the permittivity within a vacuum, R is the universal gas constant, F is Faraday's constant, T is the absolute temperature (^{o}K), V is the valence cation, and η is the electrolyte concentration. The change in the DDL due to temperature change were mainly attributed to reduction of the dielectric effect from increased temperature causing a decrease in DDL (Yueng et al. 1992, Mitchell 1993, Rowe 1998, Patel 2005). From existing literature, it was evident that a decrease in DDL thickness results in a decrease in swelling and an increase in hydraulic conductivity (Shackelford et al. 1994, 2000, Patel 2005).

The effects of temperature on permeability have been analyzed throughout research. The hydraulic conductivity increases due to the decrease in the kinematic viscosity as temperature increases. The hydraulic conductivity due to change in

temperature can be expressed as shown (Mitchel 1993, Rowe 1998, Cho et al. 1999, Ishimori and Katsumi 2012, Ozhan 2018)

$$k = \frac{K\rho g}{\mu} = K\frac{g}{v} \qquad \text{Equation 2.}$$

Where k is the hydraulic conductivity in (m/s), K is the intrinsic permeability (m^2), ρ is the permeant density (kg/m^3), μ is the permeant viscosity (Pa s), v is the kinematic viscosity (m^2/s) and g is the gravitational acceleration (9.81 m/s^2).

Cho et al. (1999), Patel (2005) and Ishimiori and Katsumi (2012) evaluated the effect of elevated temperatures on the hydraulic conductivity of mock bentonite GCLs and commercial NaB GCLs to DI water. Cho et al. (1999) investigated the effects of temperature on the hydraulic performance of compacted calcium bentonite mock GCL's to deionized water. Patel (2005) analyzed the effect of temperature (e.g., 21, 40, 60, 80, and 100 ^oC) on hydraulic conductivity of commercial NaB GCLs permeated DI water and 0.1 M $CaCl_2$ solutions. Ishimori and Katsumi (2012) analyzed the effect of elevated temperature on free swell and hydraulic conductivity of mock NaB GCLs permeated with DI water and 0.1-0.4M NaCl solutions at 20 ^oC and 60 ^oC temperatures. Results from literatures mentioned above determined main findings demonstrated an increase of hydraulic conductivity from up to one to three orders in magnitude from 20 ^oC to 100 ^oC and each literature mainly attributed change in hydraulic conductivity to change in viscosity of the permeant.

Temperature effects on hydraulic conductivity of NaB GCLs were likely to be dominated by the change of kinematic viscosity as opposed to change in swelling due to temperature change (Cho and Chun 1999, Cho et al. 1999, Patel 2005, Ishimori and

Katsumi 2012, Ye et el. 2014, Gao and Shao 2015, Ozhan 2018). Furthermore, Ishimori and Katsumi (2012) also concluded that the free swell to hydraulic conductivity relationship of NaB was not evident at elevated temperatures because the swelling of NaB, using NaCl saline solution, increased from 8.5mL/2g at 20 ^{o}C to 11mL/2g at 60 ^{o}C while the permeabilities increased from 5.9x10^{-18} m^{2} at 20 ^{o}C to2.5x10-17 m^{2}. Vryzas et al. (2017) analyzed the effect of elevated temperatures on the rheological properties of Wyoming sodium bentonite in 7% solid to DI water liquid slurry, for the purpose of understanding changes in shear stress and shear rates from an increase in temperature of slurries. Researchers concluded that the interaction between bentonite particles and water molecules become weaker as temperature of permeant solution increases and thus results in a decrease in shear resistance of the solution, providing easier flow through bentonite particles.

Ozhan (2018) evaluated the effects of elevated temperature (e.g., 20 ^{o}C, 40 ^{o}C and 60 ^{o}C) on hydraulic conductivity of mock NaB GCL, modified with either 1-2% of anionic or cationic polymer, permeated with 0.1M and 0.5M $MgCl_2$. Hydraulic conductivity of NaB GCL decreased by an order magnitude of 1.5 to 2 for all temperatures when modified with cationic polymer or anionic polymer. The 1% anionic polymer addition to NaB GCL caused the most decrease in hydraulic conductivity by 2 orders of magnitude in comparison with other enhanced GCL, however, 2% anionic polymer caused almost no reduction in permittivity when compared to 1% anionic polymer treatment. Ozhan (2018) also concluded that all the mock hydraulic conductivity GCL increased approximately an order magnitude of 2 to 2.5 as the temperature increased from 20 ^{o}C to 60 ^{o}C, which was

attributed to viscosity decrease of permeant liquid with increase in temperature. Furthermore, temperature and ionic strength of the permeant promoted a decrease in DDL of bentonite, resulting in an increase of hydraulic conductivity. However, limited information on the behavior of polymer hydrogel at elevated temperature and how would it affect the hydraulic conductivity of polymer amended bentonite were reported in this paper.

Effect of elevated temperatures on polymer hydrogel properties has been conducted and documented (Owens et al. 2007, Felix et al. 2010, Saeed 2013, Slaughter et al. 2015, Jayaramadu et al. 2019). Owens et al. (2007) analyzed thermally responsive swelling properties of both crosslinked and linear polymer networks, synthesized from acrylic acid monomers, using dynamic light scattering. Results showed that increase in temperatures resulted in a decrease in crosslinking density that resulted in an increase in final volume swelling ratio, defined as fractional increase in the mass of hydrogel due to water absorption of polymer hydrogel. Saeed (2013) analyzed the swelling properties of commercial polyacrylic acid (PAA) crosslink hydrogels as a function of temperature and found that as temperature increased, hydrogel weight and diameter increased. These results were alluded to the increase in temperature increasing the diffusion of solution, leading to an increase in overall water quantity penetrating the hydrogel. Felix et al. (2010) analyzed swell of novel crosslinked hydrogels of interpenetrating polymer networks composed of polyacrylamide and poly(γ-glutamic acid) in DI water at 25 ^{o}C and 37 ^{o}C. Jayaramadu et al. (2019) conducted swell tests on cellulose nanocrystal-based polyacrylamide crosslinked hydrogels in DI water from room temperature to 80 ^{o}C. Felix et al. (2010) and Jayaramadu

et al. (2019) found that as temperature increased, the swelling ratio of hydrogels also increased due to the dissociation of hydrogen bonding between polymer molecules occurring. The dissociation of the hydrogen bonds of interpolymer complexes, caused by an increase in temperature, increases the number of available hydrophilic sites that can interact with water molecules and also decreases crosslinking density of the hydrogel which increases the separation of polymeric chains, thus increasing the diffusion of water into hydrogels. The importance of this topic to analyze the effect of temperature on polymers can potentially assist in understanding how elevated temperatures may potentially affect the hydraulic conductivity of BPC GCLs containing either crosslinked or linear polymer.

Geng et al. (2016) analyzed the viscosity tests on bentonite-anionic polymer mixtures with DI water, $CaCl_2$, and NaCl solutions to relate viscosity of polymer-solvent solution to conformation of polymer in solution. Geng et al. (2016) concluded that contracted polymer structures result to low viscosity whereas high viscosity slurry were due to an extended polymer structure. However, researchers analyzing the change of viscosity of bentonite-liquid or BPC-liquid slurries at elevated temperatures have yet to correlate these results to change of hydraulic conductivity of GCLs. Furthermore, it was yet to be determined how BPC to liquid slurry viscosities at elevated temperatures can correlate to hydraulic conductivity of BPC GCLs at elevated temperatures. So far, limited research has comprehensively investigated the effect of temperature on hydraulic conductivity of BPC GCL to DI water and saline solution.

Objectives of this research

The objectives of this study were to investigate the effect of elevated temperatures on hydraulic conductivity of BPC GCLs and to propose characteristic changes that control the hydraulic conductivity affected by elevated temperatures. Three commercially available BPC GCLs comprising of different polymer loadings and polymer structure were exposed to DI water, 20 mM $CaCl_2$ and 50 mM $CaCl_2$ solutions at different temperatures (e.g., 20, 35, and 60 ^oC). Control test were conducted with NaB GCL. Elevated temperature tests were heated to temperatures of 35, and 60 ^oC to simulate elevated temperature gradient of a landfill. The BPC GCLs consist of either crosslinked or linear polymers. Hydraulic conductivity tests were conducted according to ASTM D6766. A heater was installed on the permeameter to achieve elevated temperature with a precision of ± 0.5 ^oC Swell index tests and viscosity tests were performed to attempt to correlate index properties to hydraulic conductivity at different temperatures. Total organic carbon (TOC) analysis was performed to evaluate the elution of polymers out of GCL samples to analyze effect of elevated temperatures on rates of polymer elution.

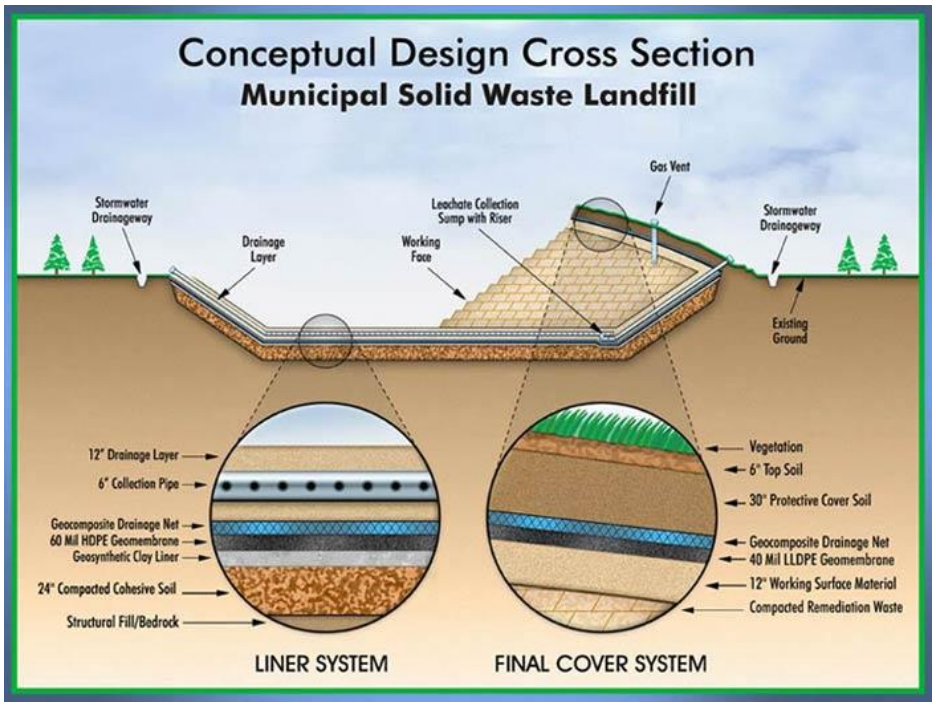

Figure 1-1. Liner system of a municipal solid waste (MSW) landfill
Source- http://www.semcolandfill.com/faq.html

CHAPTER 2

Materials

Geosynthetic Clay Liners

Three commercially available BPC GCLs (e.g., labeled as BPC1, BPC2, and BPC3) were evaluated in this study, along with a NaB GCL as controls. Polymer loading, polymer structure, and GCL mass/area can be found in Table 2-1. Grain Size Distribution can be found in Figure 2-1 along with particle size passing 10%, 30% and 60% found in Table 2-1. BPC1 and BPC2 linear polymer structure and BPC3 crosslinked polymer structure can be seen in Figure 2-2.

Permeant Solution

The permeating solutions used in experiments involved with this research were DI water, 20 mM $CaCl_2$, and 50 mM $CaCl_2$ solutions. Twenty mM $CaCl_2$ solution represents dilute landfill leachate, 50 mM $CaCl_2$ solution represents moderately aggressive solution found in landfills and DI water serves as a control solution (Tian et al 2019). Chemical property of 20 mM $CaCl_2$ and 50 mM $CaCl_2$ solutions can be found on Table 2-2. Saline solutions were produced in a 1-liter volumetric flask using DI water and calcium chloride dihydrate and stored in a plastic carboy container.

Methods

The purpose of the study was to evaluate the effect of elevated temperatures on hydraulic conductivity of BPC GCLs. Table 2-3 shows the testing matrix that was created to investigate the effect of temperature on BPC GCLs hydraulic conductivity.

Hydraulic Conductivity

GCL samples were cut from commercially manufactured rolls with a diameter of 152 mm. GCL mass and thickness were recorded for Pore Volume Flow (PVF) calculation at this stage. Geotextiles were cut to the same dimension and placed on the bottom and top of the GCL samples to distribute permeant solution. The acrylic plates, with the GCL sample, were then sealed with a latex membrane and secured using silicon (temperature resistant) O-rings to ensure prevention of side wall leakage. The hydraulic conductivity tests were performed according to ASTM D6766. Test were conducted with falling head and constant tailwater method at 20 kPa confining stress. Termination criteria was followed by ASTM 6766, in which the ratio of inflow to outflow volume must be within 0.75 and 1.25 for the last three consecutive flow measurements. Additionally, there should be no significant upward or downward trend in the hydraulic conductivity for hydraulic equilibrium to be met. Chemical equilibrium can be achieved when electrical conductivity (EC) and pH measurements of the effluent were within ±10% of the influent. The permeameter can be terminated once hydraulic and chemical equilibrium were achieved, reflecting the long-term hydraulic conductivity.

Tests were conducted at 20, 35, and 60 °C to investigate the effect of temperature on hydraulic conductivity of GCL. Heater and a thermocouple were installed in the permeameter. The temperature of permeameter was controlled by a CR10 data logger and multiplexer with a temperature accuracy of +/- 0.5 ^{o}C. Uniform heating was achieved by inserting a heat pipe with a hot water pump through the top portion of aluminum plating,

within the volume of liquid surrounding the flexible wall membrane. The permeameter was heated to target temperature before applying to confining stress.

Free Swell

The NaB and BPC samples were extracted from commercially available GCLs and carefully separated from needle-punched polypropylene nonwoven geotextiles. Free swell index tests were conducted following ASTM D5890. Two grams of bentonite or BPC were added in a 100 mL the graduated cylinder with 0.1 g increment. The graduated cylinders were initially filled with 90 mL permeant solutions. After adding the 2 g sample, the graduated cylinder will be filled to 100 mL. The swell index will be recorded after a minimum of 16 hours rest period.

The swell index standard procedure was conducted at room temperature and the elevated temperature procedure was conducted using a hot water bath apparatus. The water bath apparatus consists of a hot plate/magnetic stirrer at the base, a large metal pot placed on top, containing hot water within. The graduated cylinders filled with DI water or saline solution (e.g., 20 and 50 mM $CaCl_2$) were heated within the hot water bath prior to add bentonite. An insulating foam was used to prevent evaporation of heated water bath. The graduated cylinders were covered with parafilm to prevent evaporation of permeant within each graduated cylinder during rest time. The hot plate/magnetic stirrer and insulating foam will effectively keep the elevated temperatures accurate and consistent throughout the 16-hours.

Viscosity

Viscosity tests were performed with NaB and BPC exposed to DI water, 20, and 50 mM $CaCl_2$ solutions using a procedure outlined by Geng et al. (2016) and Vryzas et al. (2017). Oven dried NaB and BPC were added into to DI water, 20 mM $CaCl_2$, and 50 mM $CaCl_2$ solutions, specific to a solid-liquid ratio of 1:25, stirred for 5 minutes to create uniformity among bentonite particles. Cover the sample with parafilm and let rest for a minimum of 16-hours and followed by stirring the sample for no less than 30 minutes prior to measuring the sample.

The viscometer used for viscosity tests presented in this research were conducted using a ViscoQC 100. The elevated temperature viscosity tests were conducted in the same hot water bath apparatus as the swell index elevated temperature test. Initially, viscosity was measured under room temperature conditions. After measurement of the room temperature sample, samples were placed within the hot water bath to heat to 35 ^{o}C. Samples were covered with parafilm to prevent evaporation. Once the hot water bath and samples were at the desired temperature, stir the samples using a magnetic bar stirrer within the water bath for the same 30-minute stirring period and quickly measure viscosity. The same process can be repeated for samples elevated to 60 ^{o}C temperatures. It was critical to ensure the relative humidity of the surroundings be between 60% and 70% to prevent evaporation of the slurry that would inevitably increase viscosity. To mitigate this, the viscosity of the samples was recorded every 5 seconds to reduce time of test that will result in less evaporation of the slurry. Furthermore, all viscosity tests were terminated once 3

viscosity recordings remained constant. These procedures help prevent evaporation of sample and allows for proper viscosity measurements.

Total Organic Carbon Analysis

Effluent from each of the BPC GCLs was analyzed periodically for TOC analysis for the purpose of quantifying the concentration of polymer eluted. Organic carbon concentrations were analyzed using a Shimadzu TOC-L analyzer and performed according to ASTM D4839. Calibration solutions were prepared using 100 (mg/L) anhydrous potassium hydrogen phthalate. Samples were diluted 35 times to maintain the carbon content within the range of the standard calibration solution. Samples were acidified with 2 M HCl prior to being analyzed. Inorganic carbon was removed by sparging with CO_2 free gas. The remaining carbon was converted to CO2 by combusting the sample, which was then dehydrated, scrubbed to remove chlorine and other halogens, and detected for CO2 content in a nondispersive infrared gas analyzer. Polymer concentration (mg/L) in the effluent was recorded from the TOC analysis.

Fluid Loss Index

The fluid loss index test was an index test that enables the evaluation of fluid loss properties of clay mineral film or soil cake deposited onto a filter paper, which can be use to predict the hydraulic conductivity of GCL. The test procedure performed was according to ASTM D5891 for room temperature, 35 ^{o}C, and 60 ^{o}C temperature conditions. The index tests were performed from a 6% solid to liquid slurry of clay at 100 psi using a high temperature high pressure filter press cell. The procedure begins with oven dried bentonite added into saline solutions to achieve 6% solid to liquid slurry and stir for a total time of

20 minutes, poured into a separate container for a 16-hour minimum rest period. The slurry was then restirred for 5 minutes using magnetic stirrer to completely disperse the slurry. Immediately pour the entire sample slurry into the assembled filter cell and complete filter cell assembly. The total test time was 30 minutes as per the ASTM D5891; however, the first 7.5 minutes was discarded, and the data recorded from fluid loss were mL measured in the following 22.5 minutes. The volume of permeant solution that permeates through soil filter cake during the 22.5-minute was reported as fluid loss (mL).

Table 2-1. Polymer structure, polymer loading, GCL mass/area and grain size distribution of each GCL

Property	NaB	BPC1	BPC2	BPC3
Polymer Structure	-	Linear	Linear	Cross-link
Polymer Loading (%)	-	1.9	2.8	4.6
GCL Mass/Area (kg/m^3)	4.8	6.8	7.5	6.8
D10	0.4	0.2	1.75	1.75
D30	0.6	0.45	0.45	0.5
D60	1.0	0.8	0.8	0.9

Table 2-2. Chemical properties of permeant solutions

Permeant Liquid	EC (mS)	pH
DI Water	-	-
20 mM $CaCl_2$	3.93	6.3
50 mM $CaCl_2$	9.19	5.9

Table 2-3. Testing matrix for hydraulic conductivity affected by temperature

GCL	**Permeant solutions**	**Temperatures (ºC)**
NaB	DI water, 20 mM $CaCl_2$, 50 mM $CaCl_2$	20, 35, 60
BPC1	DI water, 20 mM $CaCl_2$, 50 mM $CaCl_2$	20, 35, 60
BPC2	DI water, 20 mM $CaCl_2$, 50 mM $CaCl_2$	20, 35, 60
BPC3	DI water, 20 mM $CaCl_2$, 50 mM $CaCl_2$	20, 35, 60

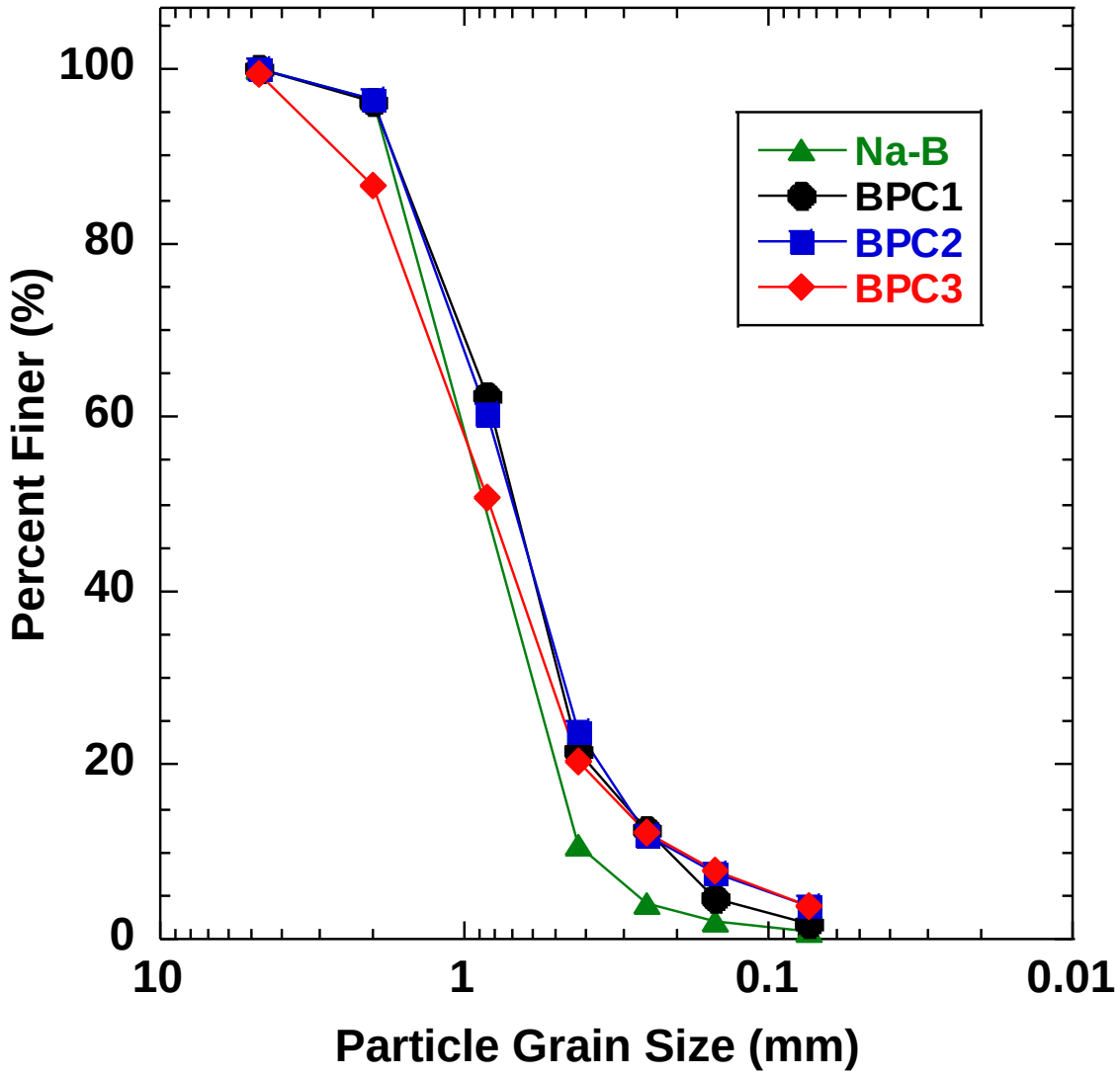

Figure 2-1. Grain size distribution for each GCL used.

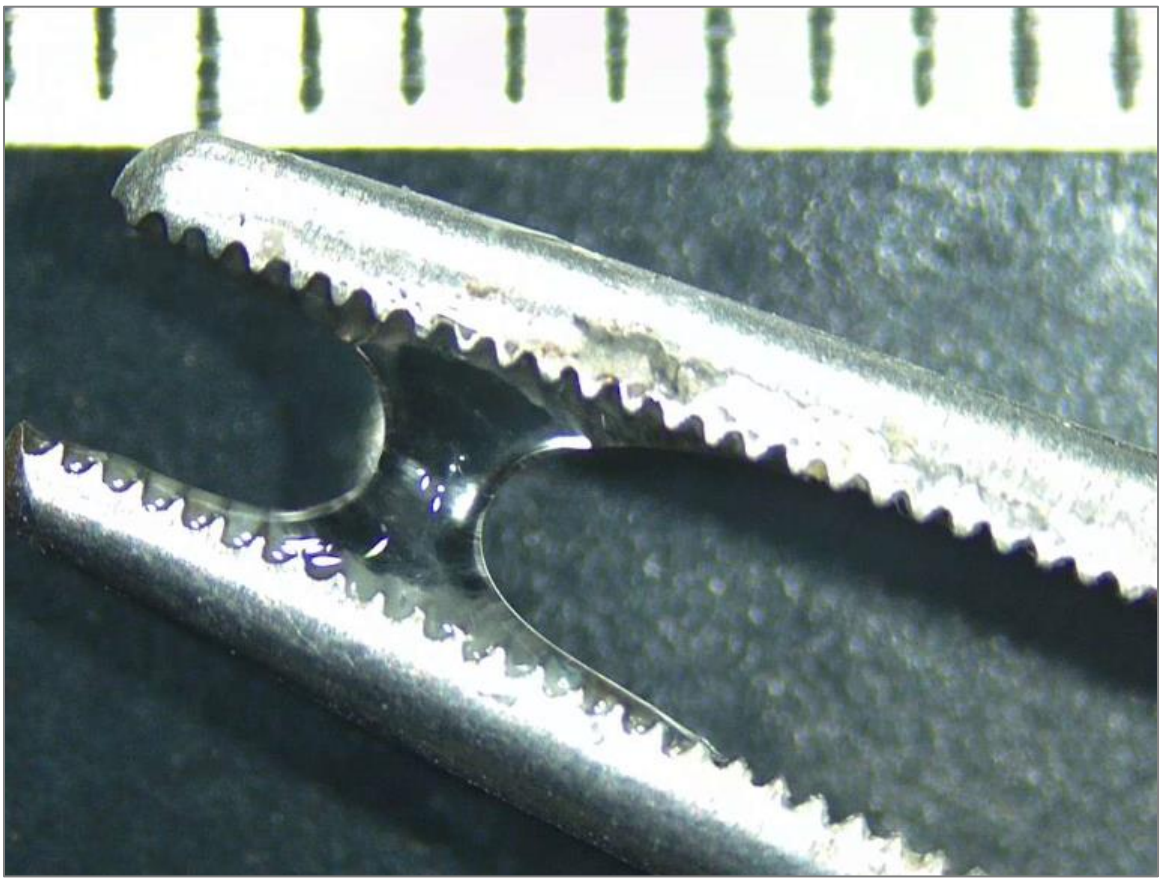

(a)

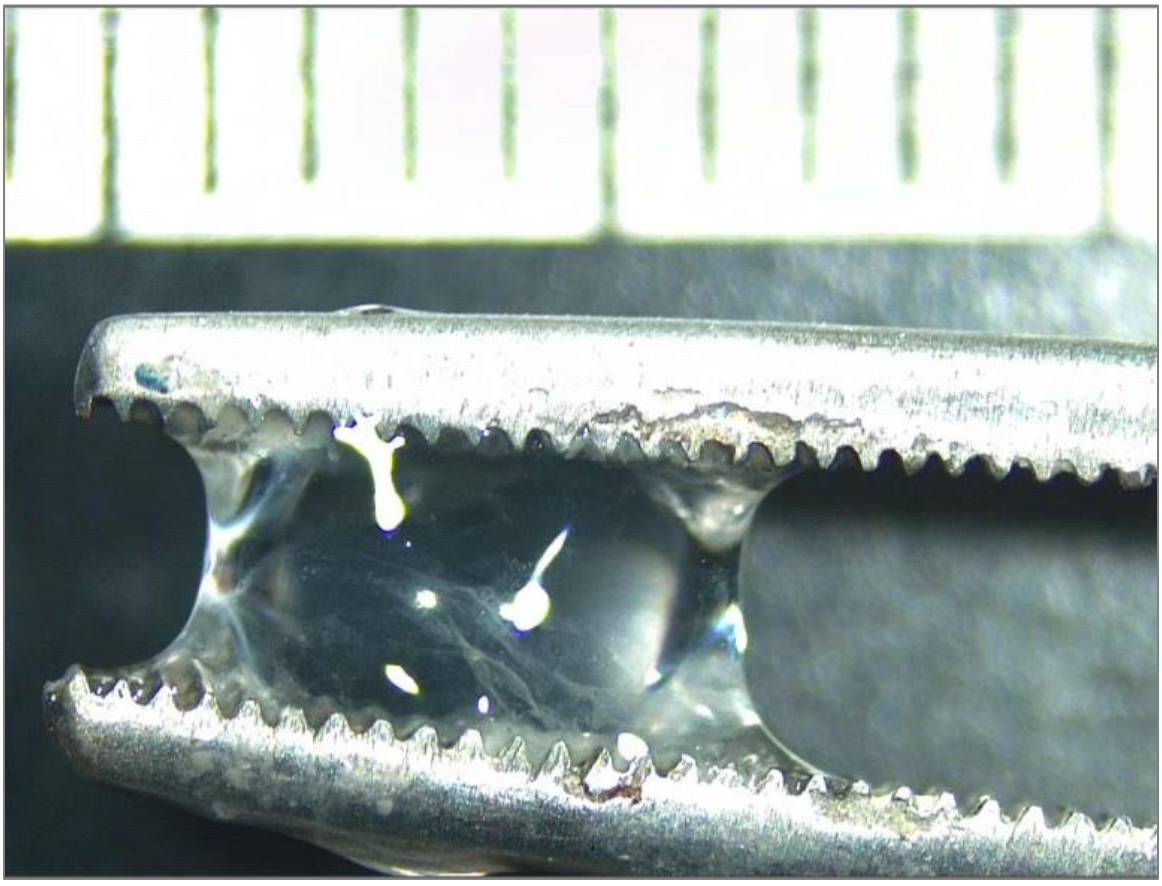

(b)

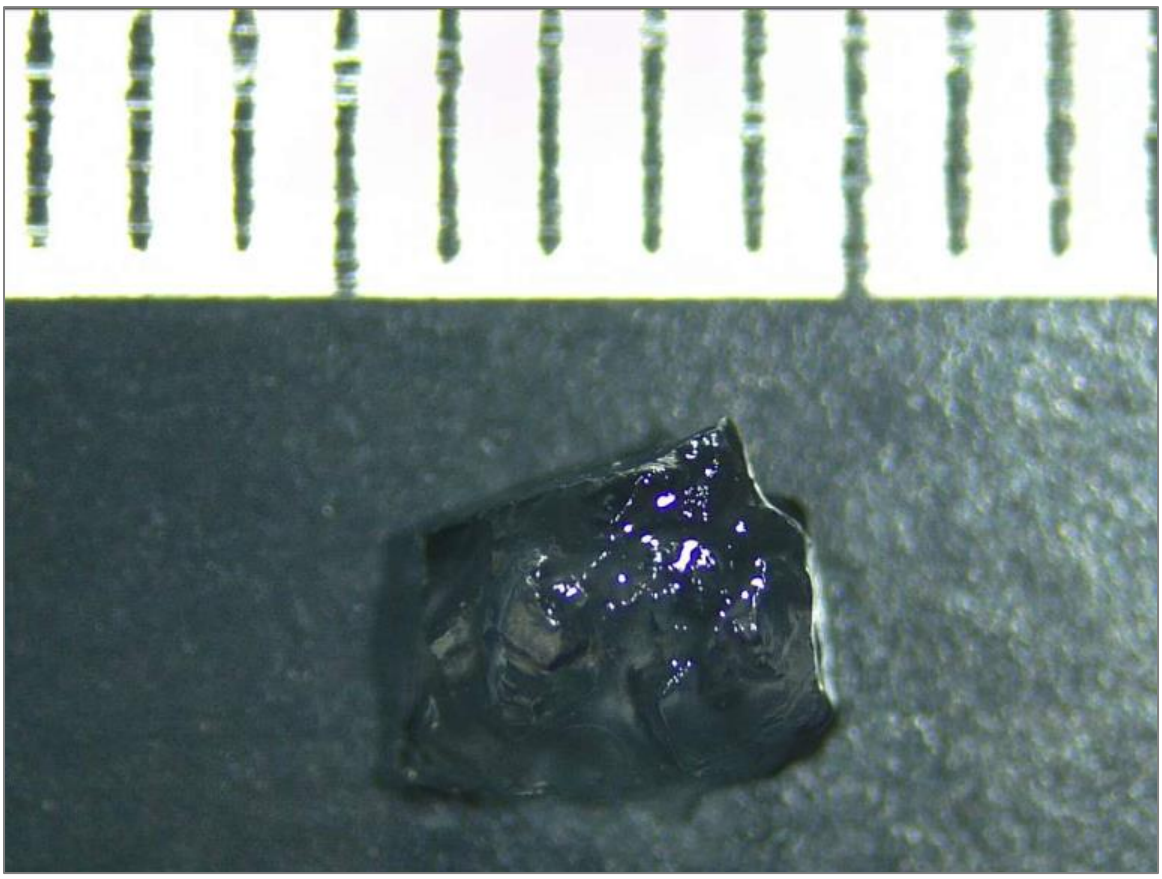

(c)

Figure 2-2. Linear Polymer structure of (a)BPC1, (a) BPC2 and crosslink polymer structure of (c) BPC3. Length scale in mm.

CHAPTER 3

Results and discussion

Table 3-3 summarizes results of the hydraulic conductivity tests. The BPC GCLs permeated with 50 mM $CaCl_2$ solutions meet all of the termination criteria according to ASTM D6766. The BPC GCLs permeated with 20 mM $CaCl_2$ and DI water had not met all of the termination criteria and are still permeating until the hydraulic and chemical equilibrium are reached. Test on the BPC GCLs permeated with DI water and 20 mM $CaCl_2$ solutions were still ongoing.

Swelling Index

Swell indices of NaB and each of the BPC GCLs are shown in Figure 3-1 as a function of temperature. The swell index of the conventional NaB in DI water decreased with increasing temperature from 28mL/2 g at room temperature to approximately 26 mL/2 g at 60 ^{o}C. The reduction in swell index was caused by decrease in DDL as a function of temperature increase of liquid solution (Yueng et al. 1992, Shackelford 1994, Patel 2005, Ishimori and Katsumi 2012). Swell indices in DI water have a much larger swell compared to 50 mM $CaCl_2$ saline solution and were attributed to osmotic swell occurring in DI water. Ionic strength of the dilute and moderately aggressive 20 mM $CaCl_2$ and 50 mM $CaCl_2$ solutions prevent osmotic swell from occurring thus resulting in a reduced swell index as compared to DI water. Swell indices for BPC GCLs in DI water, 20 mM, and 50 mM $CaCl_2$ solution are shown in Figure 3-1. The test result show swell index increased as temperature increase from 20 to 60 ^{o}C. These findings suggest that the swelling of polymer increased

as the temperature increased, which is opposite than that of NaB. Furthermore, BPC GCL with higher polymer loading had a larger increase of swell. This phenomenon of both crosslinked and linear polymers experiencing a higher swell when induced with elevated temperatures is observed in existing literature and occurs from dissociation of hydrogen bonds providing more hydrophilic sites to attach to more water molecules (Owens et al. 2007, Felix et al. 2010, Saeed 2013, Slaughter et al. 2015, Jayaramadu et al. 2019).

Viscosity

Viscosity of DI water, 20 mM $CaCl_2$, and 50 mM $CaCl_2$ saline solutions as temperature increases can be found in Table 3-1. As temperature increases the viscosity of each permeant solution decreased as the rheological properties of the solution become more free flowing from a reduction in internal friction (Wang et al. 2016, Vryzas et al. 2017).

Viscosity of solid to liquid slurries as a function of temperature can be found in Figure 3-2. NaB solid to liquid slurry shows an increase in viscosity compared to pure permeant viscosity. This result suggests that the NaB does influence viscosity of saline solutions from the result of particle-to-particle frictional resistances. However, as temperature is increased the interaction between bentonite particles and DI water molecules become weaker and results in a decrease in particle-to-particle frictional resistances. Additionally, the BPC viscosity results were larger than the NaB viscosity, suggesting that the polymers also influence particle-to-particle frictional resistances to increase viscosity of solid to liquid slurries. Each of the NaB and BPC solid to liquid slurries decrease in viscosity as temperature was increased. Decrease in viscosity of the BPC can potentially

indicate a decrease in polymer binding to NaB resulting in a reduction in particle-to-particle friction and resulting in a decrease in viscosity as temperature was increased.

Hydraulic Conductivity

Typical data from a hydraulic conductivity test are shown in Figure 3-3 for BPC1 GCL permeated with 50 mM $CaCl_2$ solution at 35 ^oC. Hydraulic conductivity increases from a PVF of 1 to about 18 PVF when hydraulic equilibrium was reached with five consistent hydraulic conductivity readings. EC stabilized at approximately 5 PVF, within the ASTM termination criteria, and stabilized throughout the remainder of permeation. Ph stabilized at approximately 7 PVF when evaluating pH with the same criteria as EC of the effluent. Chemical equilibrium was reached when the EC and pH were stabilized within criteria.

Final hydraulic conductivity of all the tests can be found in Table 3-3. For NaB GCLs permeated with DI water, hydraulic conductivity has small reduction in hydraulic conductivity as temperatures were increased. This is attributed to the swell index results of NaB in DI water being very large measurements for both room temperature and elevated temperature, thus preventing hydraulic conductivity of NaB to experience an effect in elevated temperatures. Whereas, NaB swell in 50 mM CaCl2 saline solution prevents osmotic swelling and results in smaller swell index values at room temperature and at 60 ^oC which allows the elevated temperatures to affect hydraulic conductivity of NaB. Hydraulic conductivity of NaB permeated by 50 mM $CaCl_2$ was seen to gradually increase as temperature increased. Hydraulic conductivity of both BPC1 and BPC2 GCLs in DI water at 60 ^oC decreased compared to room temperature due to the increase in hydrogel

swelling as temperatures were increased. The crosslink BPC3 GCL experienced small increase in hydraulic conductivity permeated with DI water, however this increase is negligible considering the very low hydraulic conductivity measurements. Each of the BPC GCLs showed an increase in hydraulic conductivity as temperature increased when permeated with 50 mM $CaCl_2$. Both of the linear GCLs BPC1 and BPC2 experienced increase in hydraulic conductivity as opposed to the crosslinked BPC3 GCL. Hydraulic conductivity of BPC1 permeated with 50 mM $CaCl_2$ increased from $2.33x10^{-8}$ (m/s) at room temperature to $4.48x10^{-8}$ (m/s) at 60 ^{o}C. Additionally, the hydraulic conductivity of BPC2 permeated with 50 mM $CaCl_2$ increased from $1.19x10^{-08}$ (m/s) at room temperature to $3.68x10^{-08}$ (m/s) at 60 ^{o}C. Comparing hydraulic conductivity results of 50 mM $CaCl_2$ to DI water results for both BPC1 and BPC2 can allude to the possibility of polymer eluting from the GCL samples at elevated temperatures. The hydraulic conductivity of the crosslinked BPC3 GCL permeated with 50 mM $CaCl_2$ decreased minimally from $3.88x10^{-11}$ (m/s) at room temperature to $2.46x10^{-11}$ (m/s) at 60 ^{o}C. Hydraulic conductivity for both linear BPC GCLs increased by more than 2-fold when temperature was increased to 60 ^{o}C, compared to the crosslink BPC3 GCL that decreased at elevated temperatures. A comparison of the final hydraulic conductivity measurements for each of the GCLs permeated with DI water, and 50 mM CaCl2 at each temperature can be found in Figure 3-4.

Hydraulic conductivity trend for both BPC1 and BPC2 linear GCLs permeated by 50 mM $CaCl_2$ can be seen on Figure 3-5. BPC1 GCL trends show that increase in temperatures can cause an initial reduction in hydraulic conductivity by approximately 1

to 2 orders in magnitude at low PVF. Similarly, it can be seen in Figure 3-5 (b) the linear BPC2 GCL had an initial low hydraulic conductivity to 50 mM $CaCl_2$ mM solution (~$1.13x10^{-12}$ m/s) at elevated temperature than that that of BPC2 at room temperature (~$1.19x10^{-8}$ m/s). Both reductions in hydraulic conductivity for BPC1 and BPC2 may potentially be alluded to swell index increase as temperature was increased for linear BPC GCLs. Katsumi et al. (2008) analyzed relationship between hydraulic conductivity of bentonites and free swell at a confining pressure of 30kPa. It was found that hydraulic conductivities of bentonites with a free swell greater than 15 (mL/2 g) resulted in a hydraulic conductivity of approximately $1x10^{-11}$ (m/s). Additionally, Zainab et al. (2021) analyzed relationships of swell index to hydraulic conductivity of six BPC GCLs modified with either crosslinked and linear polymers permeated by aggressive saline solutions and DI water. Researchers determined that at a swell index of approximately 16 (mL/2 g) for five out of six of the BPC GCLs resulted in hydraulic conductivities lower than $1x10^{-10}$ (m/s). From Fig. 3-1 (b) it can be seen that at room temperature BPC3 was the only BPC GCL that has a swell index greater than 15 (mL/2 g) at room temperature. However, at 60 ^oC the swell index of linear BPC GCLs increased to 15 (mL/2 g) or greater thus resulting in a decreased hydraulic conductivity at elevated temperatures compared to room temperature during the initial permeation.

From Figure 3-5, it can be seen that the final hydraulic conductivity values for both BPC1 and BPC2 are larger than the initial hydraulic conductivities at low PVF. The final hydraulic conductivity for BPC1, 50 mM $CaCl_2$ at 60 ^oC, is $4.48x10^{-8}$ (m/s) compared to initial hydraulic conductivity of $1.2x10^{-11}$ (m/s). Additionally, the final hydraulic

conductivity of BPC2, 50 mM $CaCl_2$ at 60 ^oC, is $3.68x10^{-8}$ (m/s) compared to hydraulic conductivity of $1.13x10^{-12}$ (m/s) at low PVF. Furthermore, it can be deduced that the increase in temperature can potentially cause linear polymers to be squeezed out of the GCL sample because of the increase in swelling of the polymers within the GCL specimen as temperature is increased.

Polymer Elusion

Total organic carbon analysis results can be seen in Figure 3-6 for each GCL permeated with 50 Mm $CaCl_2$ for room temperature, 35 ^oC (-BPC1), and 60 ^oC. It can be seen from Figure 3-6 (a) that BPC1 GCL shows higher concentrations of TOC at elevated temperatures compared to room temperature. Similarly, Figure 3-6 (b) shows the TOC concentrations for BPC2 at room temperature and 60 ^oC. The TOC at 60 ^oC shows more rapid rates of polymer elusion through the GCL sample compared to the room temperature TOC analysis. However, in Figure 3-6 (c) the TOC analysis for the crosslinked BPC3 GCL shows the opposite trend as the linear BPC GCLs. It can be noted that the crosslinked GCL elutes less polymers at elevated temperatures, compared to room temperature polymer elusion, as opposed to the relationship shown for both linear BPC GCLs in which more polymers are eluted at elevated temperatures.

As can be seen from Figure 3-7 (a), and (b), linear BPC2 GCLs show an increase in rates of polymer elution as temperature was increased. The polymer elusions greatly affected hydraulic conductivity of both linear BPC GCLs, however, more so in the BPC2 GCL with increased polymer loading. From Figure 3-7 (a) it can be seen that the hydraulic conductivity increases gradually from $4x10^{-13}$ (m/s) to $4x10^{-8}$ (m/s), and this was attributed

to the polymer eluting from the GCL and thus reducing beneficial effects from polymers. Additionally, the BPC1 GCL also showed larger cumulative TOC of approximately 9000 (mg/L) at 60 ^{o}C as opposed to approximately 5600 (mg/L) at room temperature. Furthermore, as a result of the of polymer elusion, the BPC1 GCL at 60 ^{o}C increased gradually from $1.2x10^{-11}$ (m/s) to final hydraulic conductivity at $3.68x10^{-8}$ (m/s). As can be seen from Figure 3-8, the rate at which polymer elutes for linear BPC GCLs increased as a result from increased temperatures. Thus, the hydraulic conductivity of linear BPC GCLs will increase as a result of more rapid polymer elution at elevated temperatures.

As can be seen from Figure 3-9, the effect of temperature on the polymer elution of crosslinked BPC GCL shows the opposite relationship as the linear BPC GCLs. In comparison, crosslink hydrogels within BPC3 GCL were physically constrained gel structures that were not liquid soluble, as opposed to the linear BPC GCLs. Crosslink polymer structure can be seen in Figure 2-2 (c). As temperature was increased crosslink hydrogels increase in swelling as a result. From Table 3-2, the hydrogel mass was observed to have larger swell capacity at larger temperatures and thus increases in size. However, because of the physical nature of the crosslink hydrogels, these hydrogels were more likely to be trapped in between intergranular spaces as swelling increases. Thus, resulting in a more rapid polymer elution occurring at room temperature as opposed to elevated temperatures. Additionally, the hydraulic conductivity of BPC3 GCL at room temperature steadily increases as more polymer was eluted as opposed to the 60 ^{o}C test that begins to be consistent at 15 PVF. However, the overall effect of temperature increase has little effect on hydraulic conductivity of the crosslink BPC3 GCL. This can be mainly attributed to the

polymer loading of the BPC3 GCL having the largest polymer loading of the BPC GCLs thus showing that more polymers must be eluted to have more effect on the hydraulic conductivity of crosslink BPC3 GCL.

The relationship between hydraulic conductivity and TOC for each BPC GCL permeated with 50 mM $CaCl_2$ saline solution can be found in Figure 3-10. The relationship for linear BPC GCLs shows that at elevated temperatures the polymer elutes more rapidly out of a GCL, resulting in larger hydraulic conductivity as opposed to a lower hydraulic conductivity at room temperature. BPC1 GCL at room temperature has a cumulative TOC of approximately 5600 (mg/L) with a hydraulic conductivity of 2.33×10^{-8} (m/s). Whereas, at 60 ^{o}C, the BPC1 GCL has a cumulative TOC of approximately 9000 (mg/L) with a hydraulic conductivity of 4.48×10^{-8} (m/s). BPC2 GCL follows the same trend starting with a cumulative TOC of 4900 (mg/L) with a hydraulic conductivity of 1.19×10^{-8} (m/s) at room temperature and a cumulative TOC of 9600 (mg/L) with a hydraulic conductivity of 3.68×10^{-8} (m/s) at 60 ^{o}C. Both the linear BPC GCLs show an increase in hydraulic conductivity and eluted TOC with respect to increase in temperatures. The BPC3 GCL hydraulic conductivity has little change with respect to temperature change. The hydraulic conductivity of BPC3 at room temperature was 3.88×10^{-11} (m/s) with an eluted cumulative TOC of 11,000 (mg/L) whereas the 60 ^{o}C has a hydraulic conductivity of 2.46×10^{-11} (m/s) with an eluted TOC of 3200 (mg/L). The hydraulic conductivity was larger at room temperature because of the increased amount of TOC eluted due to crosslink hydrogels at room temperature being smaller in size as compared to the size of hydrogels at elevated temperatures that would experience larger swelling.

Table 3-1- Viscosity of permeant solutions at 20, 35 and 60 ^{o}C temperatures.

Permeant Viscosity (mPa-s)			
Temperature(^{o}C)	DI water	20 mM $CaCl_2$	50 mM $CaCl_2$
20	1.198	1.576	1.318
35	0.719	1.037	1.018
60	0.479	0.677	0.959

Table 3-2- Hydrogel mass change at 20, 35 and 60 ^{o}C temperatures in DI water and 50 mM $CaCl_2$.

Polymer	Leachate	Temperature (^{o}C)	Trial 1	Trial 2	Trial 3	Trial 4	Average (mg)
			Swell (mg)	Swell (mg)	Swell (mg)	Swell (mg)	
Crosslinked	DI water	23	18.80	14.50	23.90	14.51	17.93
		35	35.40	23.60	45.60	19.80	31.10
		60	41.80	45.00	48.80	26.20	40.45
	50mM$CaCl_2$	23	4.10	3.80	3.30	3.80	3.75
		35	4.80	4.10	3.60	4.70	4.30
		60	5.10	5.00	4.00	4.90	4.75

Table 3-3. Hydraulic conductivity of each GCL permeated by DI water, 20 mM $CaCl_2$ and 50 mM $CaCl_2$ at 20, 35 and 60 ^oC.

GCL	Leachate	Temperature (^oC)	PVF	Termination Criteria Satisfied?		Hydraulic Conductivity (m/s)	Swell Index (mL/2 g)	Viscosity (mPa-s)	Fluid Loss (mL)
				Hydraulic Equilibrium	Chemical Equilibrium				
NaB	DI water	20		Yes	Yes	4.30E-11	28.00	5.93	5.25
		60	14.01	No	No	1.75E-11	26.50	4.07	7.10
	20mM $CaCl_2$	20	15.07	Yes	Yes	3.85E-08	17.50	4.25	
		35	20.53	Yes	Yes	1.58E-08	17.25	3.66	
		60	24.55	Yes	Yes	1.50E-08	17.00	2.22	
	50mM $CaCl_2$	20		Yes	Yes	1.40E-07	11.00	4.01	31.30
		35	17.90	Yes	Yes	1.63E-07	10.50	3.18	34.00
		60	20.39	Yes	Yes	2.17E-07	10.00	2.94	58.20
BPC1	DI water	20	2.26	No	Yes	3.75E-12	28.00	11.26	2.95
		60	2.04	Yes	Yes	1.04E-12	34.00	9.80	4.10
	20mM $CaCl_2$	20	2.64	No	No	4.96E-12	18.00	10.42	
		60	2.01	No	No	2.73E-11	21.00	9.43	
	50mM $CaCl_2$	20	25.21	Yes	Yes	2.33E-08	12.00	7.13	22.70
		35	19.68	Yes	Yes	5.46E-08	12.50	6.87	30.23
		60	21.69	Yes	Yes	4.48E-08	15.00	6.38	62.03

GCL	Leachate	Temperature (°C)	PVF	Termination Criteria Satisfied?		Hydraulic Conductivity (m/s)	Swell Index (mL/2 g)	Viscosity (mPa-s)	Fluid Loss (mL)
				Hydraulic Equilibrium	Chemical Equilibrium				
BPC2	DI water	20	4.23	Yes	Yes	3.39E-12	30.00	33.07	3.10
		60	1.22	No	Yes	6.96E-13	35.50	25.67	3.88
	20mM $CaCl_2$	20	7.62	No	No	4.40E-12	19.50	12.76	
		60					22.50	10.48	
	50mM $CaCl_2$	20	24.4	Yes	Yes	1.19E-08	13.00	9.67	11.75
		35	3.97	No	No	1.93E-12	14.00	9.16	14.23
		60	25.6	Yes	Yes	3.68E-08	16.50	8.64	52.00
BPC3	DI water	20	5.89	No	Yes	3.80E-12	41.00	31.45	3.00
		60	10.9	Yes	Yes	5.85E-12	45.50	29.11	4.97
	20mM $CaCl_2$	20	3.70	No	No	4.64E-12	25.50	7.49	
		60					29.50	9.53	
	50mM $CaCl_2$	20	30.6	Yes	Yes	3.88E-11	17.50	5.81	17.77
		35	24.8	No	Yes	2.60E-11	18.00	5.33	21.90
		60	26.5	Yes	Yes	2.46E-11	19.00	4.97	35.33

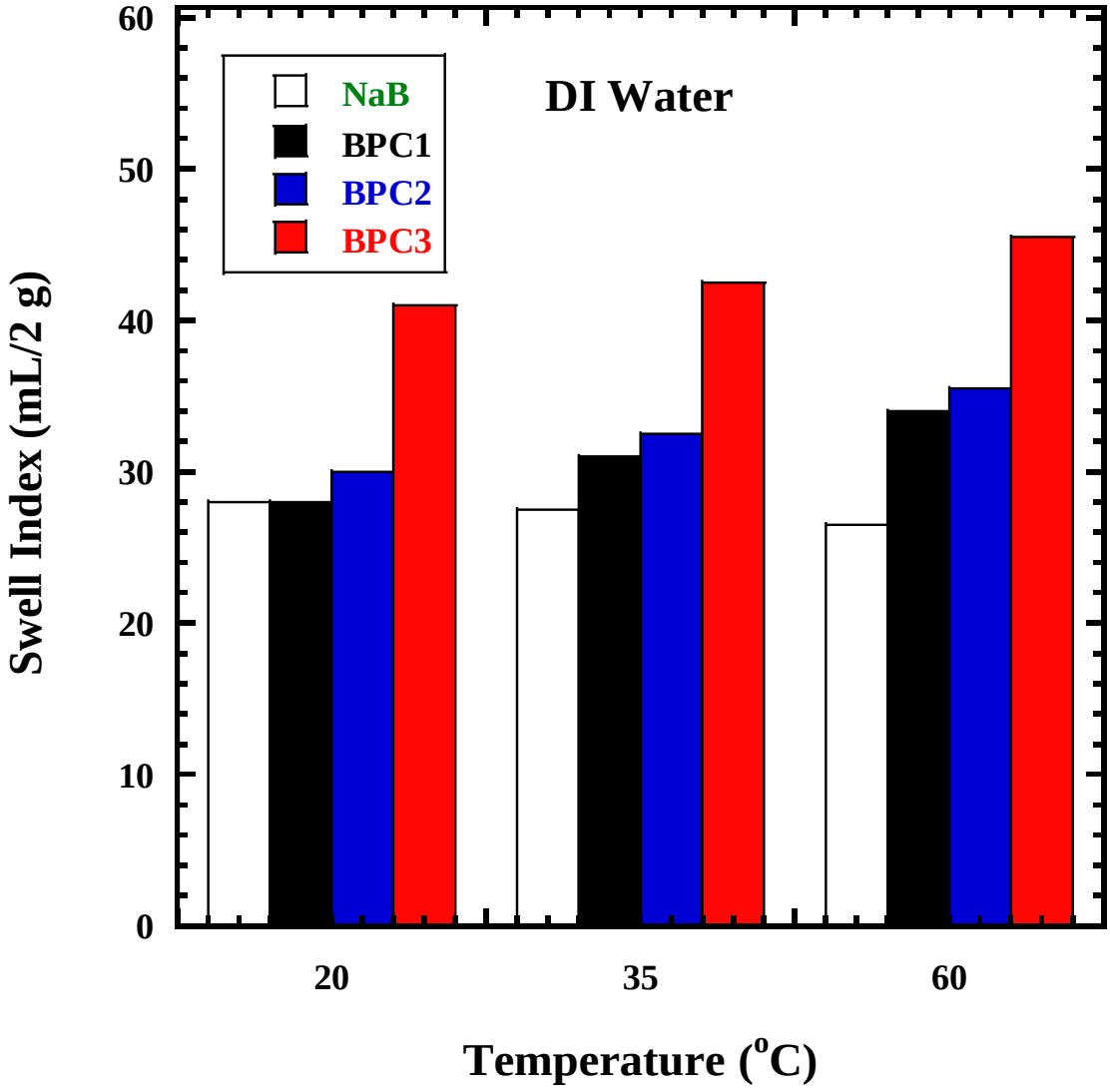
DI Water
NaB
BPC1
BPC2
BPC3
Swell Index (mL/2 g)
0
10
20
30
40
50
60
20
35
60
Temperature (°C)

(a)

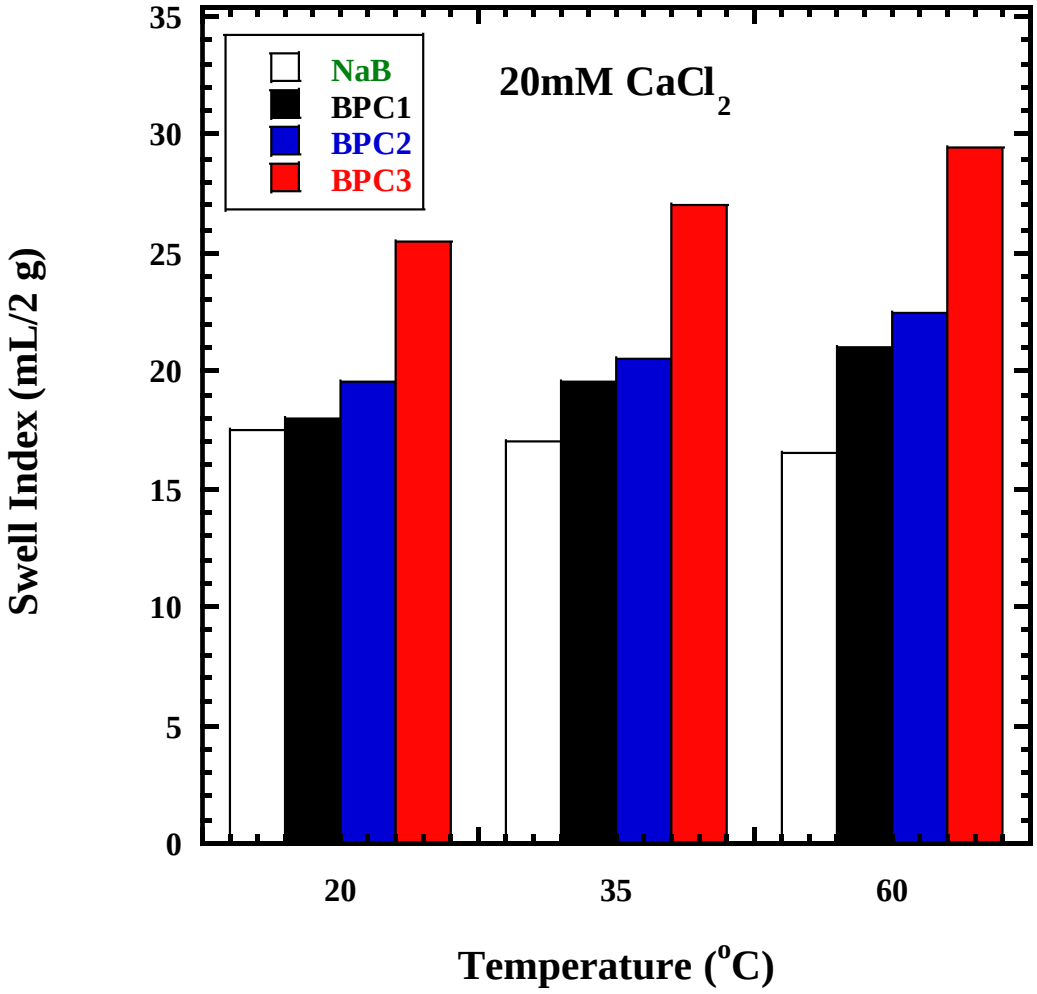
NaB
BPC1
BPC2
BPC3
20mM CaCl2
Swell Index (mL/2 g)
Temperature (°C)
0
5
10
15
20
25
30
35
20
35
60

(b)

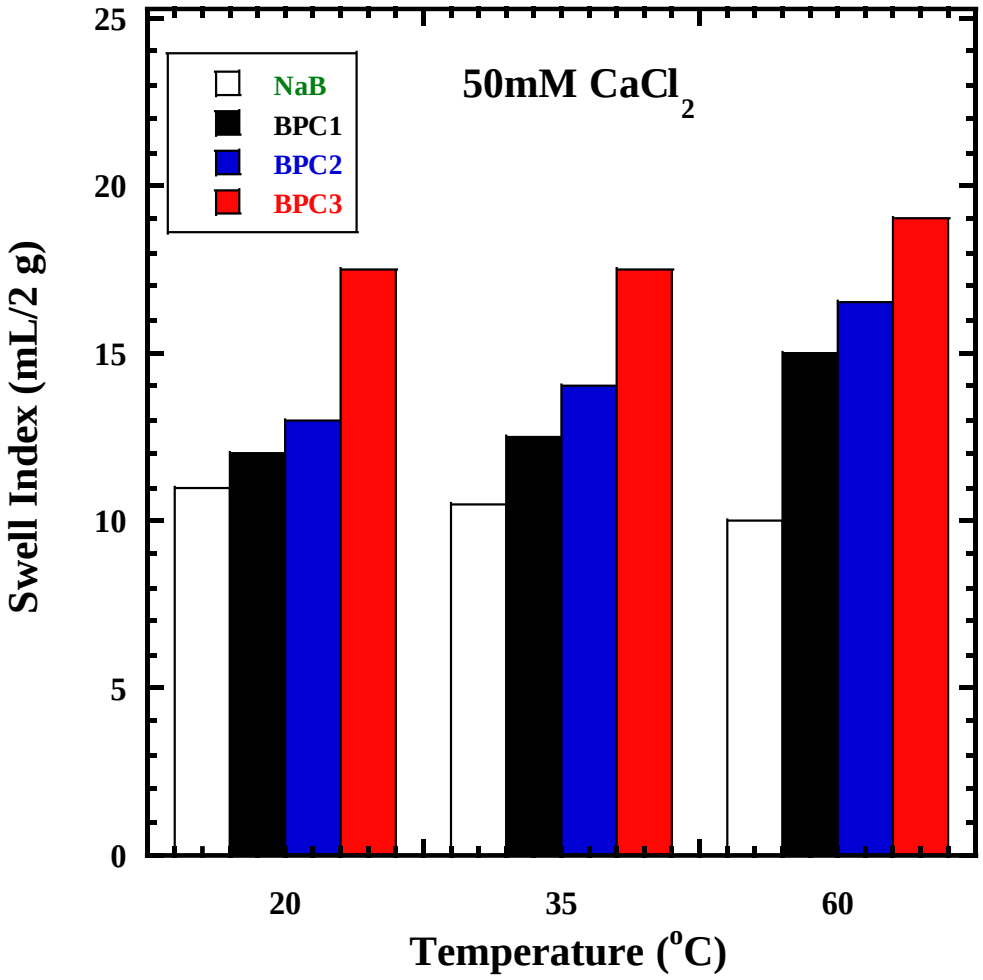

(c)

Figure 3-1. Swell index of Na-B and BPCs using (a) DI water, (b)- 20 mM $CaCl_2$, (c)- 50 mM $CaCl_2$.

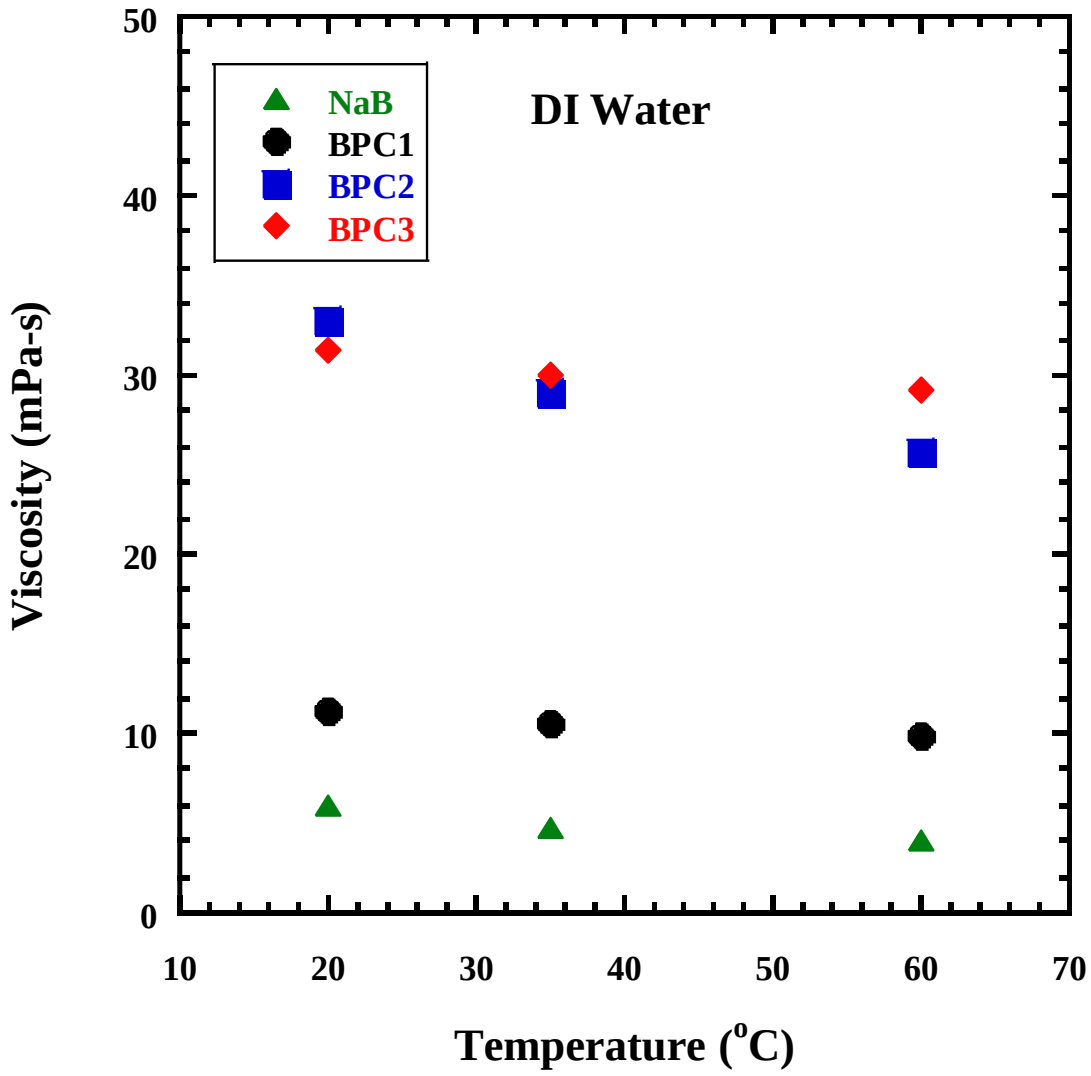
DI Water
NaB
BPC1
BPC2
BPC3
Viscosity (mPa-s)
Temperature (°C)
0
10
20
30
40
50
10
20
30
40
50
60
70

(a)

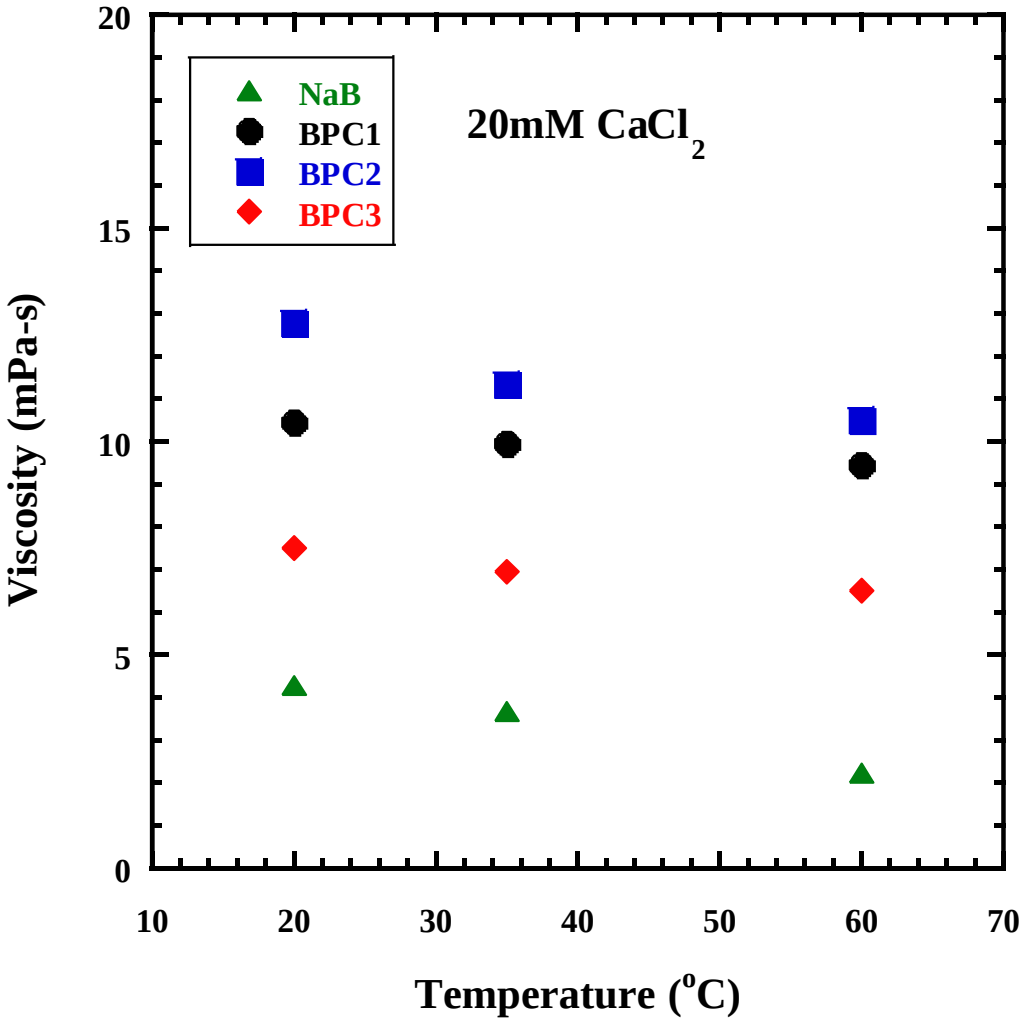
20
15
10
5
0
Viscosity (mPa-s)
NaB
BPC1
BPC2
BPC3
20mM CaCl2
10
20
30
40
50
60
70
Temperature (°C)

(b)

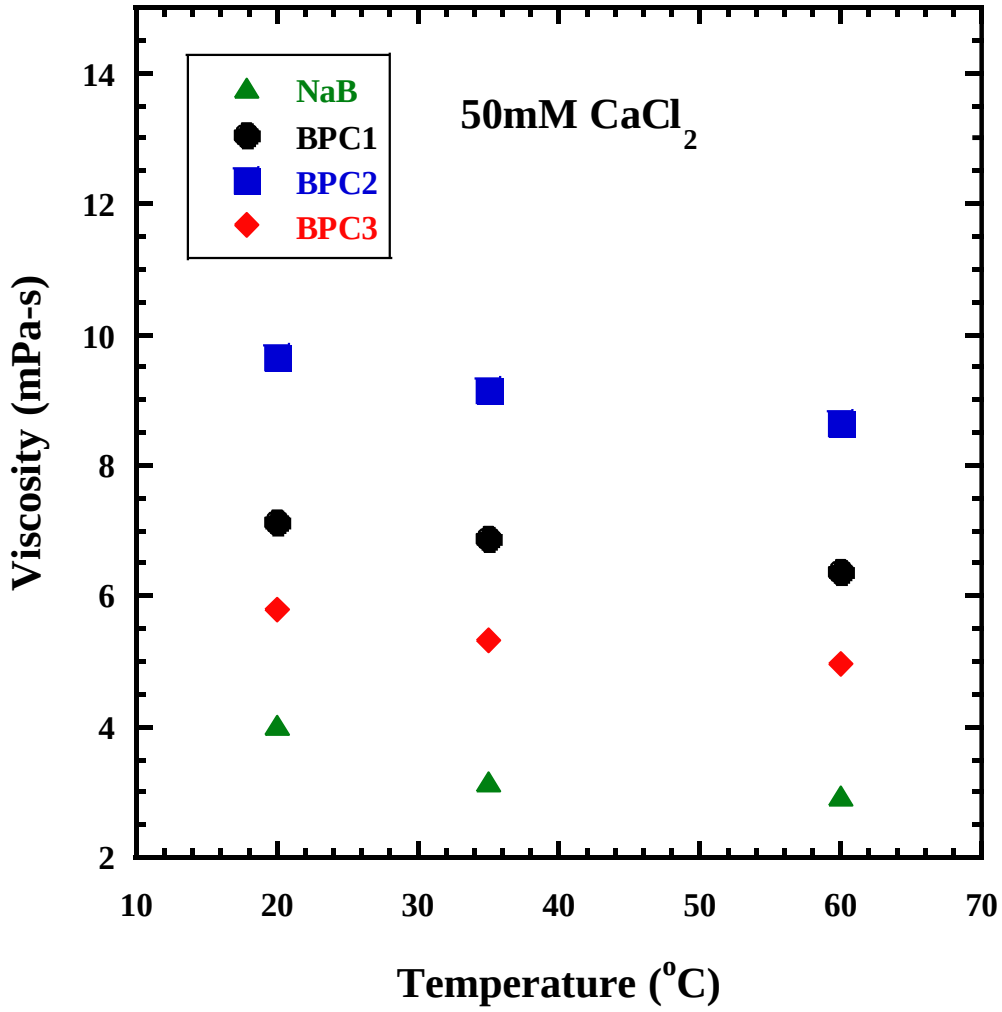

(c)

Figure 3-2. Viscosity of 4% solid to saline solution slurries of NaB and BPC at 20, 35 and 60 ºC in (a) DI water, (b) 20 mM $CaCl_2$, (c) 50 mM $CaCl_2$.

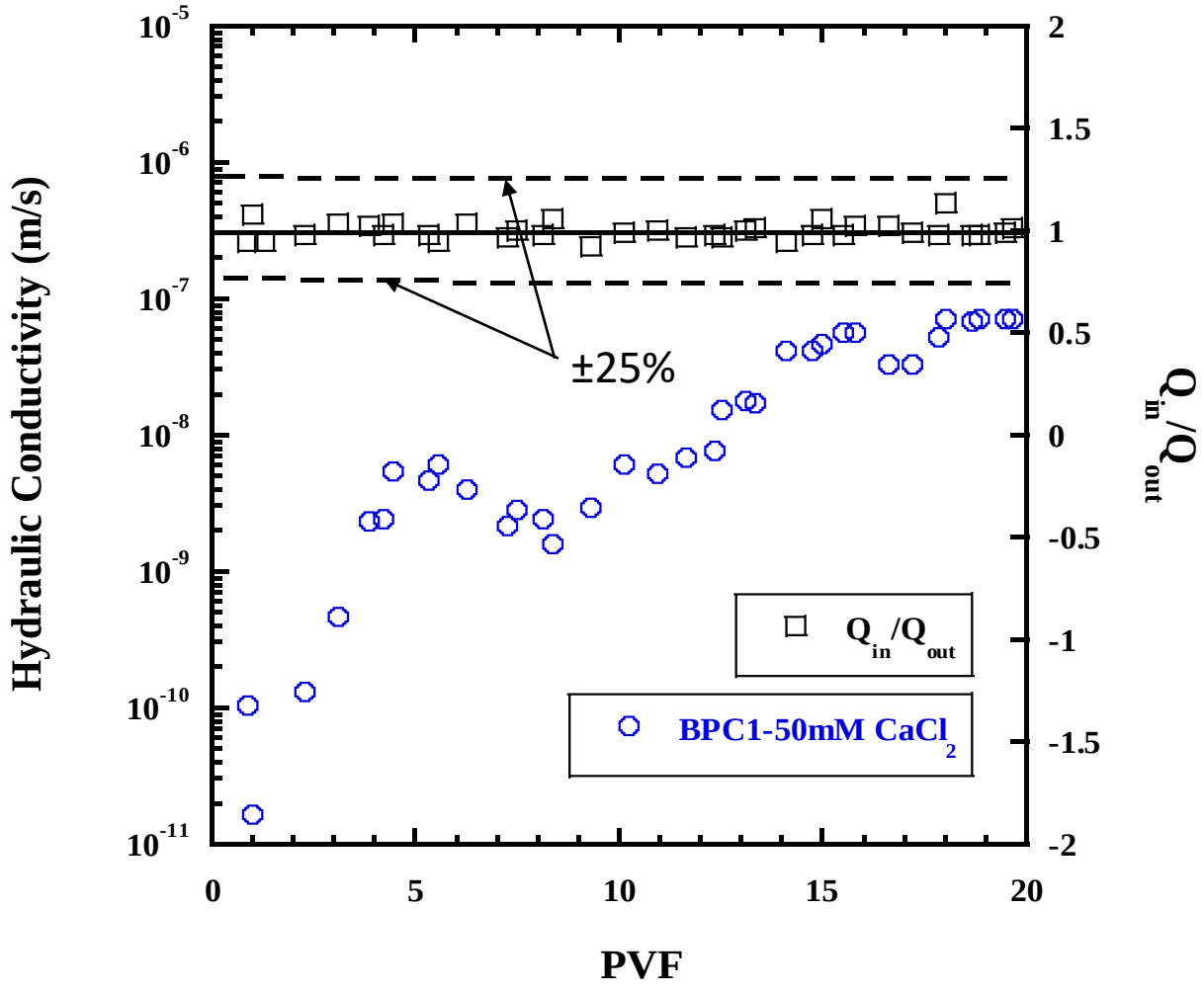
Hydraulic Conductivity (m/s)
10-5
10-6
10-7
10-8
10-9
10-10
10-11
2
1.5
1
0.5
0
-0.5
-1
-1.5
-2
0
5
10
15
20
PVF
Qin/Qout
±25%
Qin/Qout
BPC1-50mM CaCl2

(a)

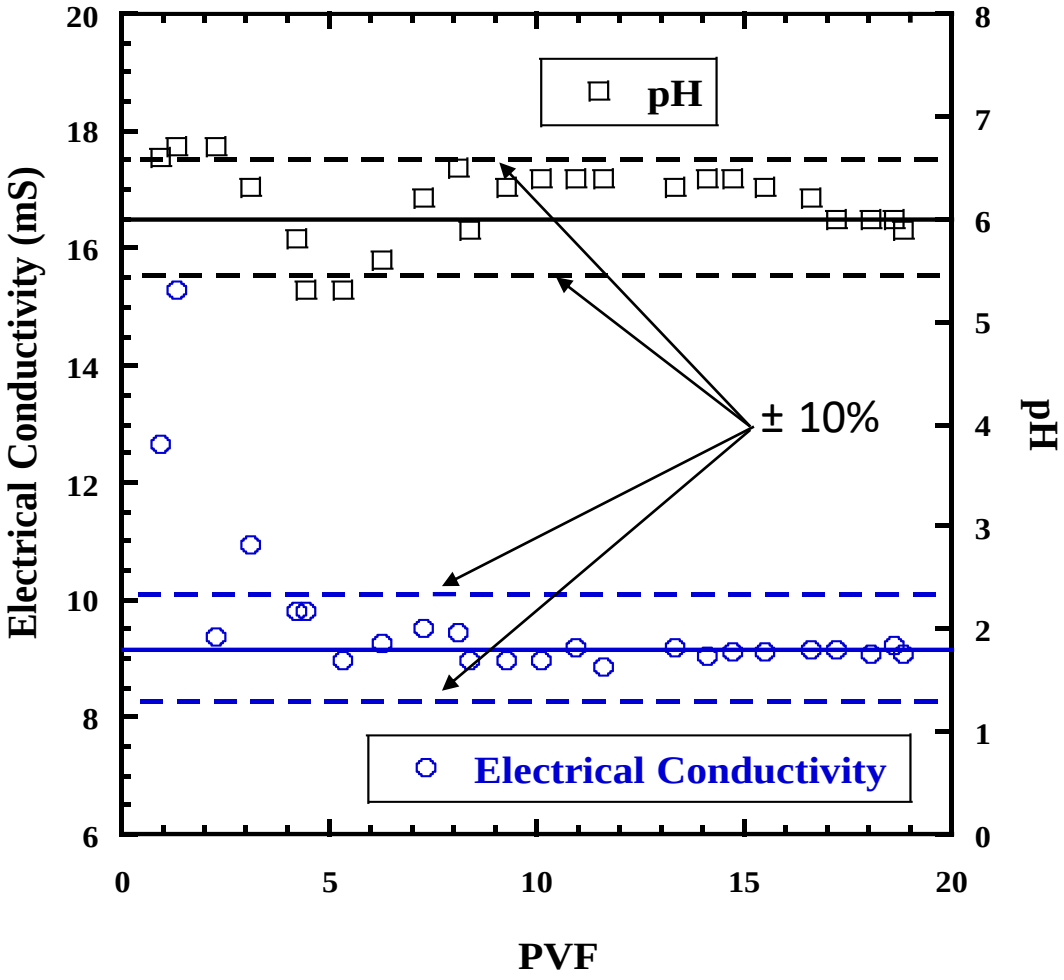

(b)

Figure 3-3. Hydraulic conductivity and ratio of inflow to outflow of (a) BPC1 GCL at 35 ^{o}C permeated with 50 mM $CaCl_2$ saline solution, (b) pH, and EC of effluent.

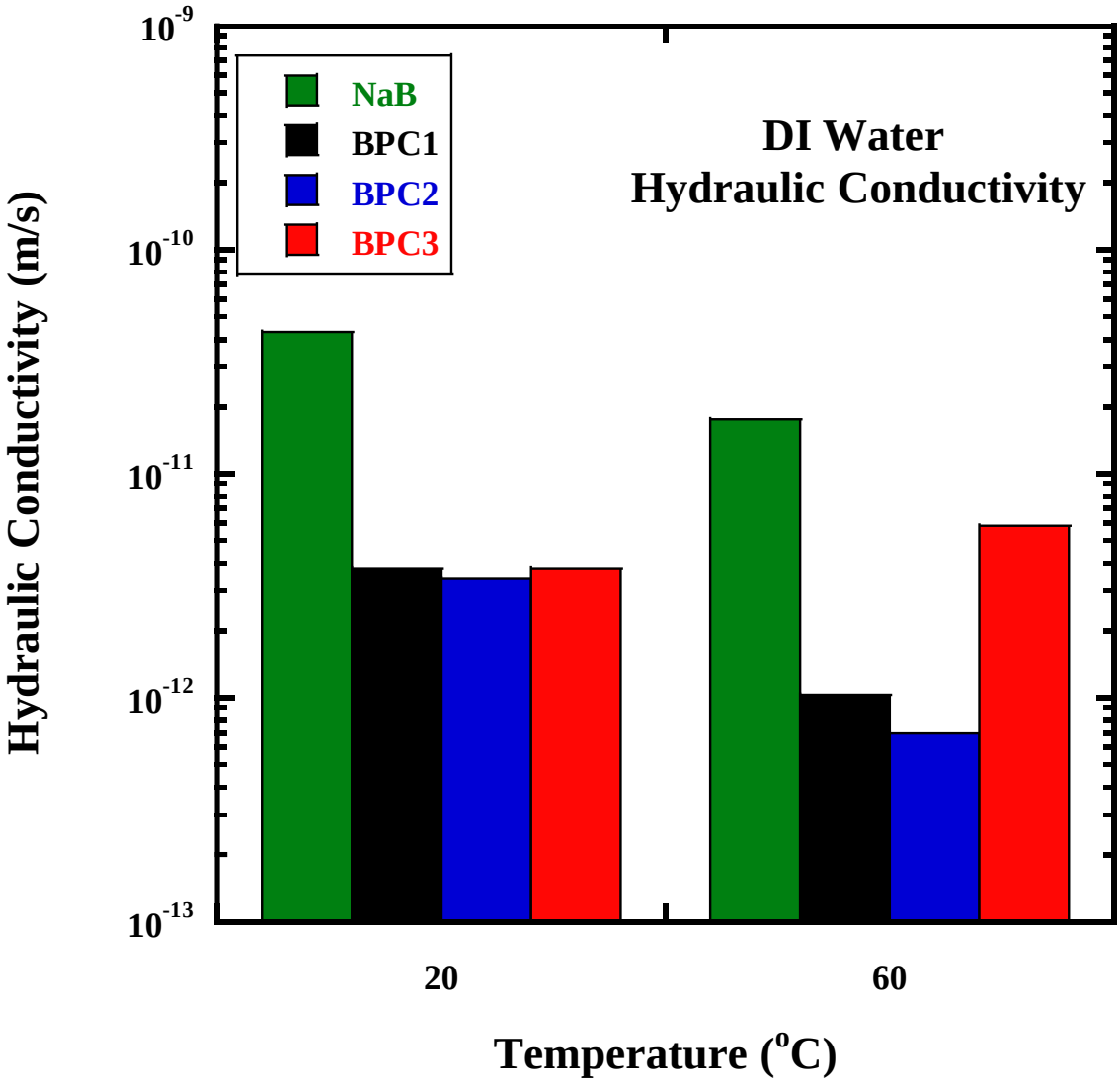
Hydraulic Conductivity (m/s)
10-9
10-10
10-11
10-12
10-13
NaB
BPC1
BPC2
BPC3
DI Water
Hydraulic Conductivity
20
60
Temperature (°C)

(a)

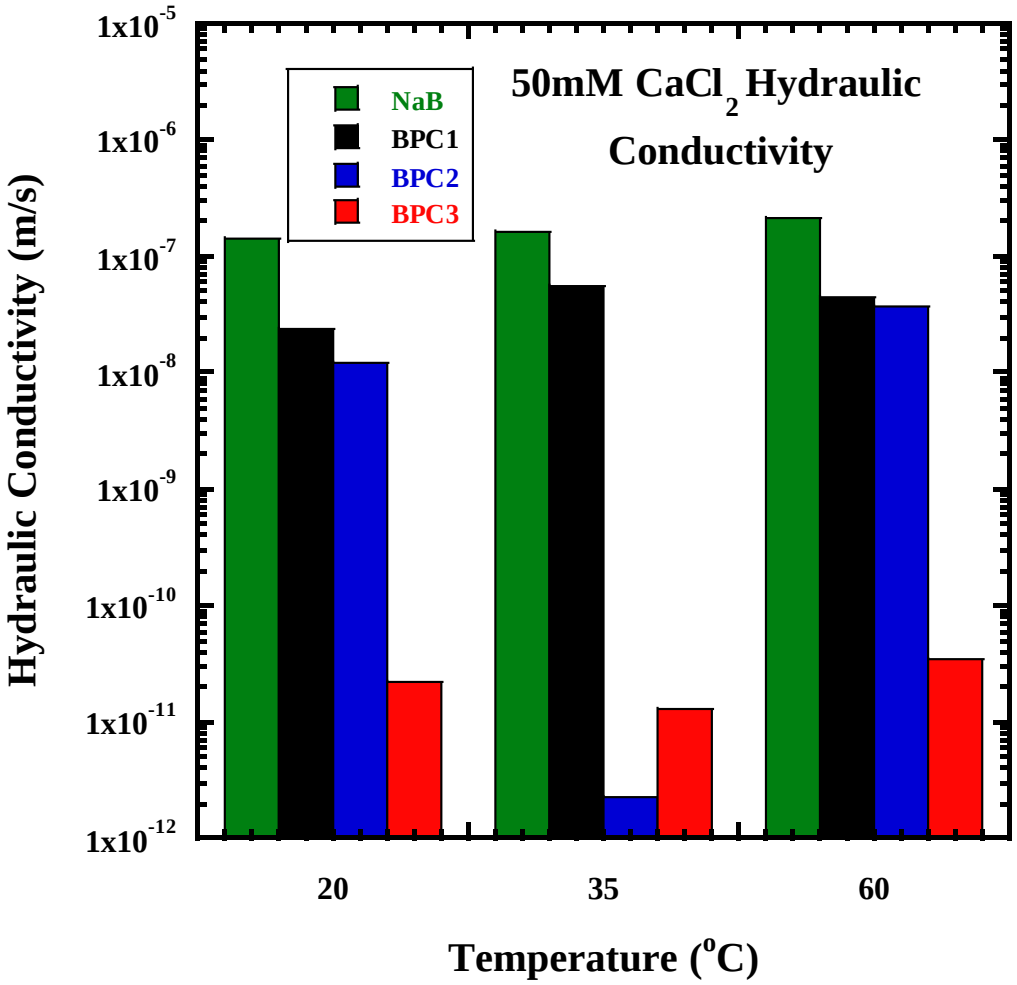

(b)

Figure 3-4. Hydraulic conductivity of BPC1, BPC2, BPC3 permeated by (a) DI water at 20 and 60 ºC and (b) 50 mM $CaCl_2$ at 20, 35, 60 ºC.

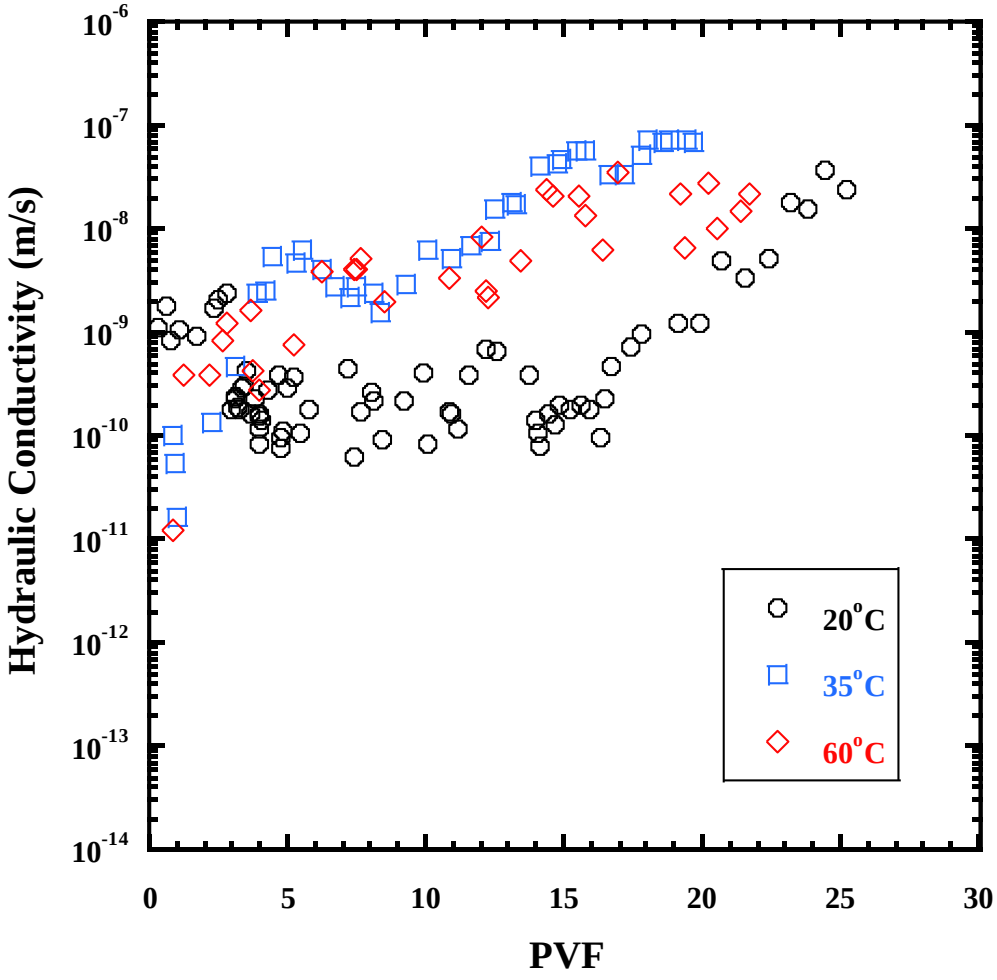
Hydraulic Conductivity (m/s)
10-6
10-7
10-8
10-9
10-10
10-11
10-12
10-13
10-14
0
5
10
15
20
25
30
PVF
20°C
35°C
60°C

(a)

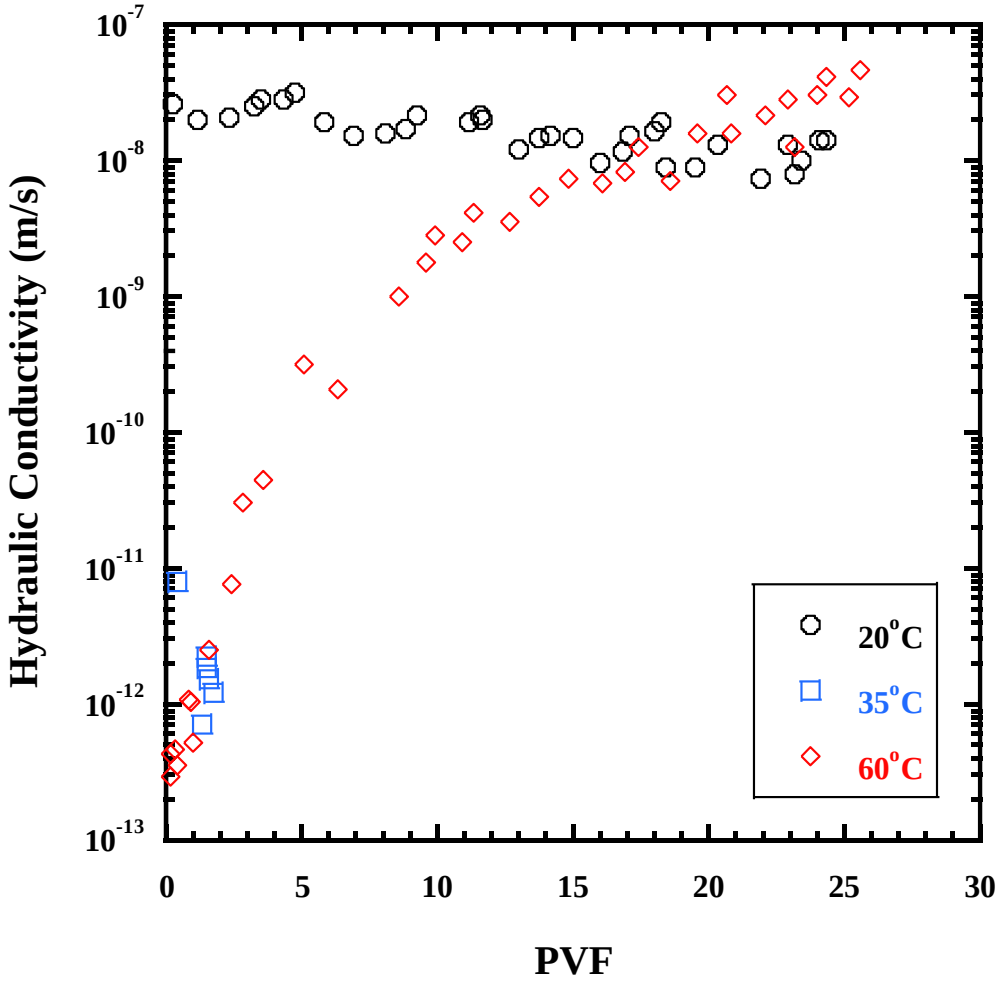

(b)

Figure 3-5. Hydraulic conductivity of (a) BPC1 and (b)BPC2 GCL permeated with 50 mM $CaCl_2$ at 20, 35, and 60 °C.

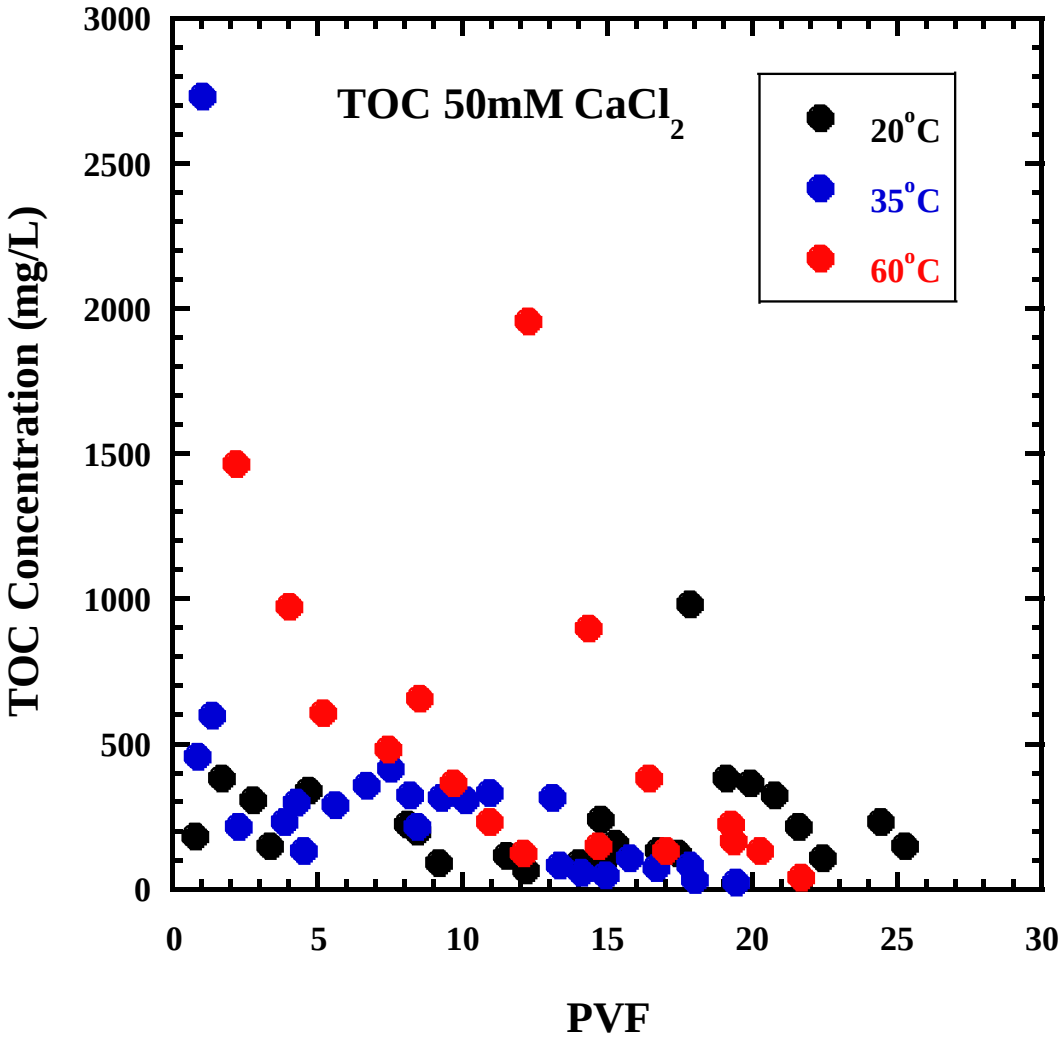
TOC 50mM CaCl2
20°C
35°C
60°C
TOC Concentration (mg/L)
PVF
0
500
1000
1500
2000
2500
3000
0
5
10
15
20
25
30

(a)

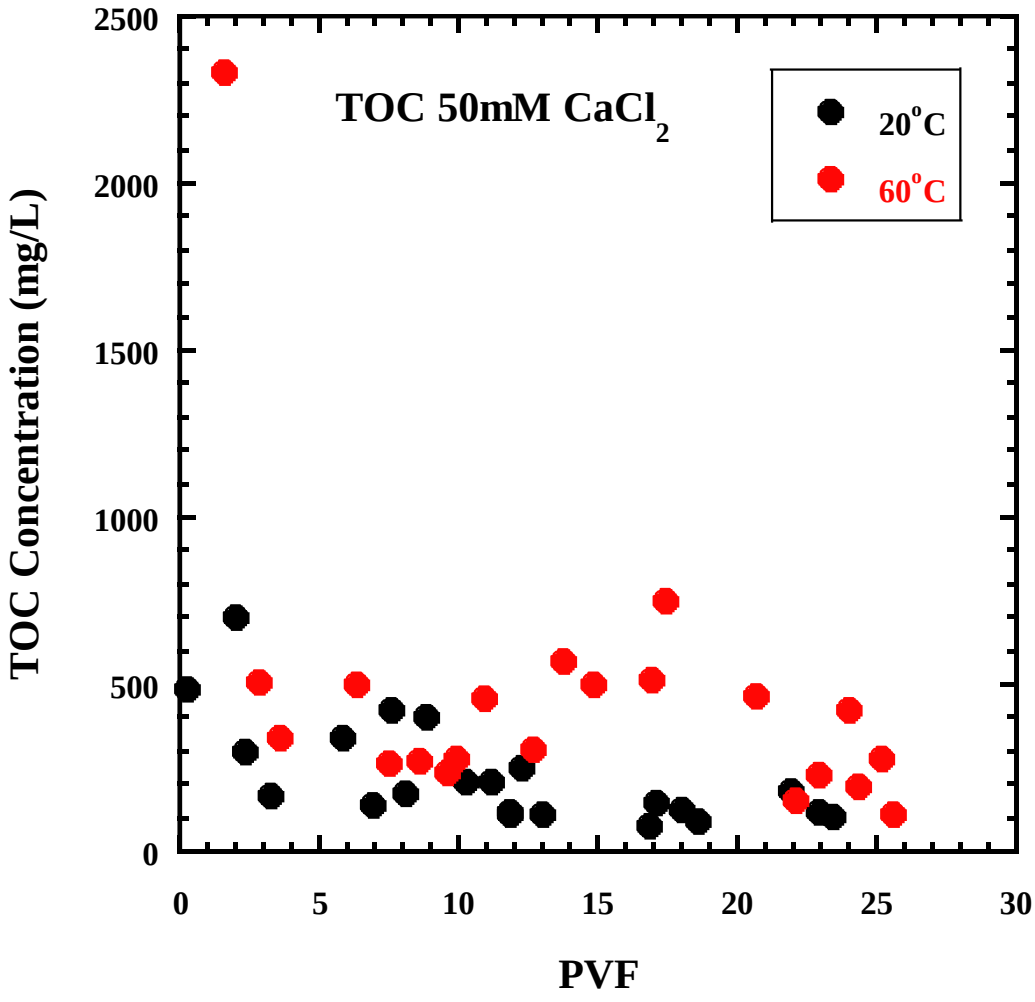
TOC 50mM CaCl2
20°C
60°C
TOC Concentration (mg/L)
PVF
2500
2000
1500
1000
500
0
0
5
10
15
20
25
30

(b)

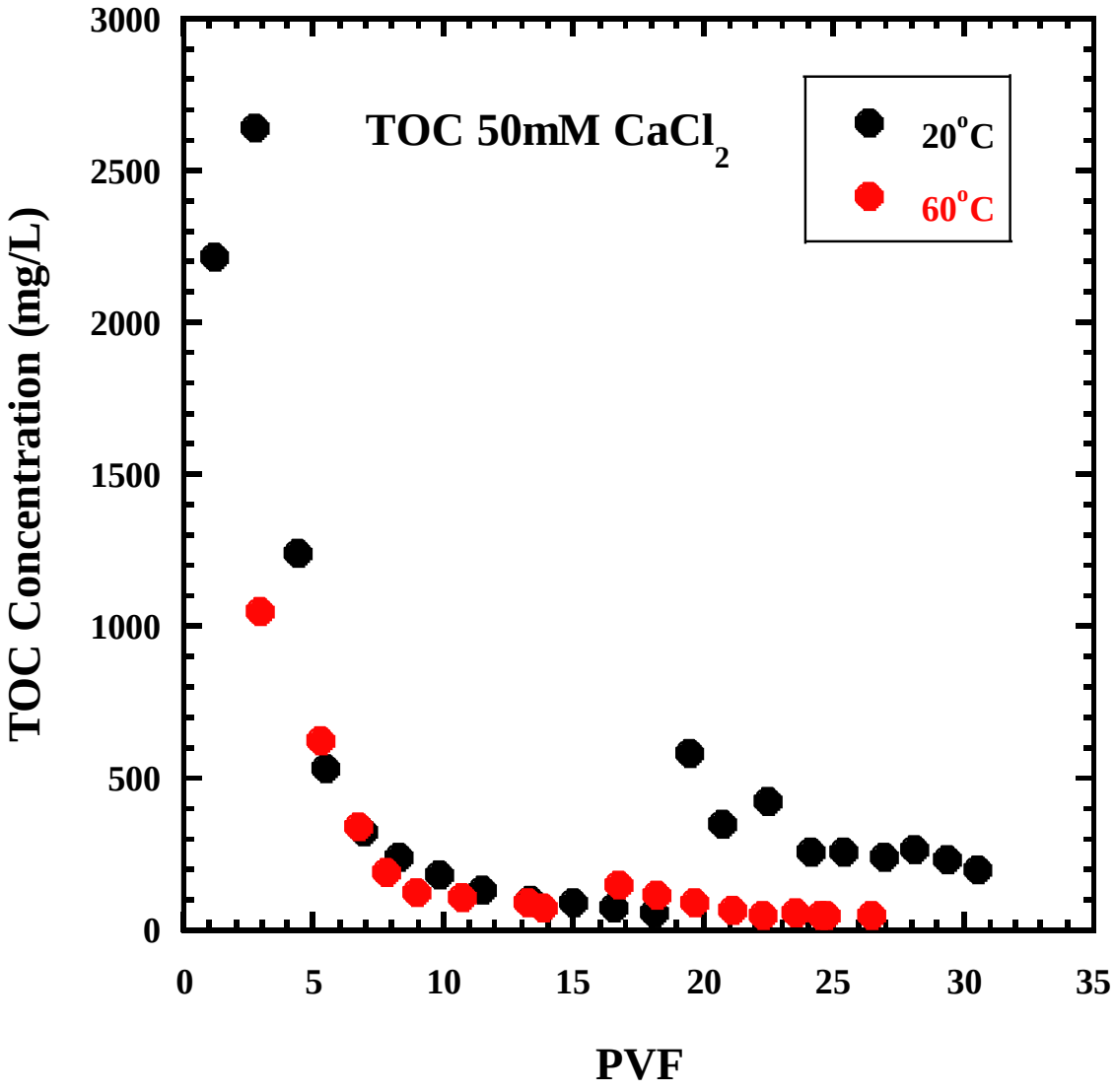

(c)

Figure 3-6. TOC concentration (mg/L) of (a) BPC1, (b) BPC2, (c) BPC3 at 20,35, and 60 °C permeated by 50 mM $CaCl_2$.

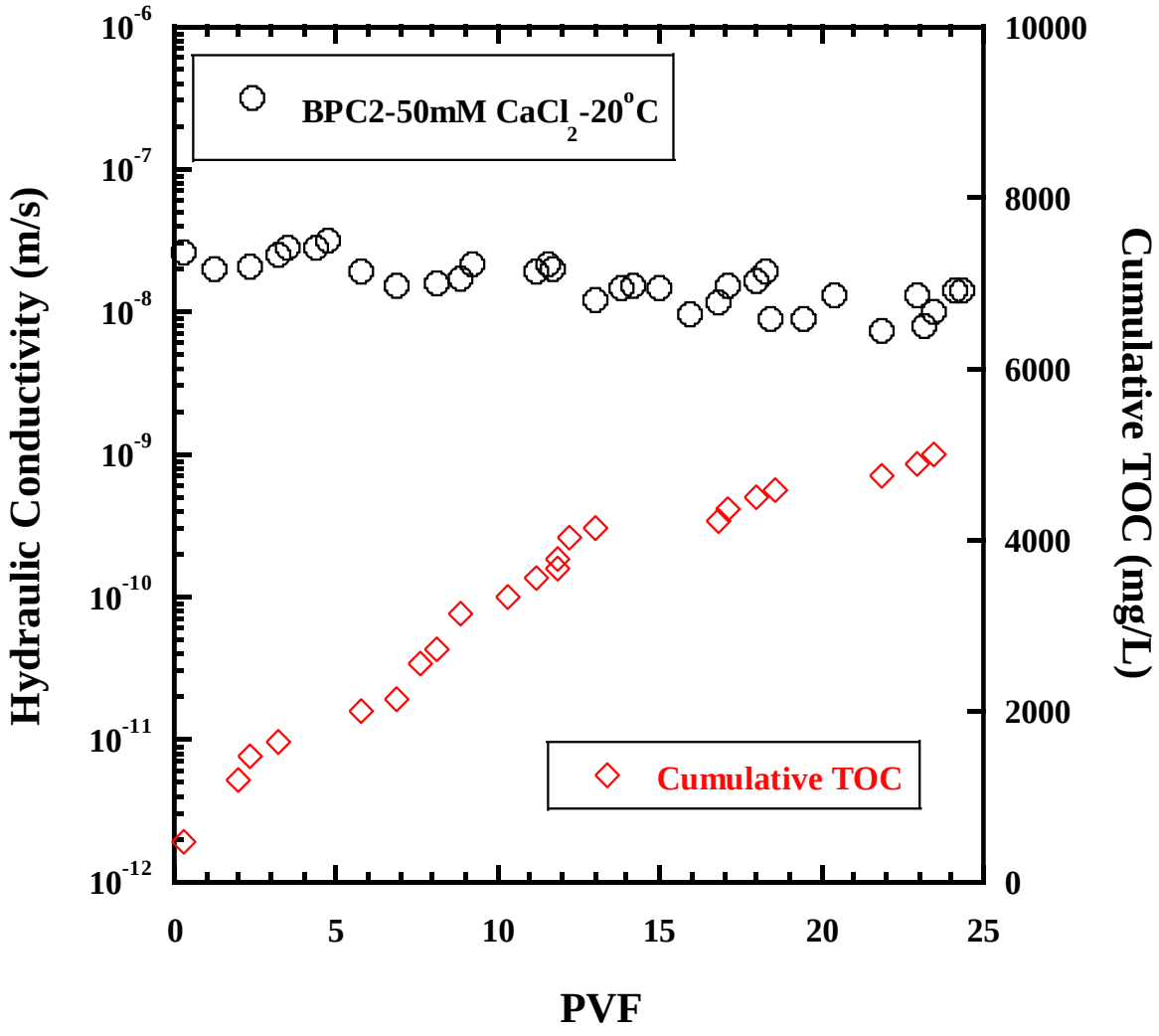
BPC2-50mM CaCl2-20°C
Cumulative TOC
Hydraulic Conductivity (m/s)
Cumulative TOC (mg/L)
PVF
10-6
10-7
10-8
10-9
10-10
10-11
10-12
10000
8000
6000
4000
2000
0
0
5
10
15
20
25

(a)

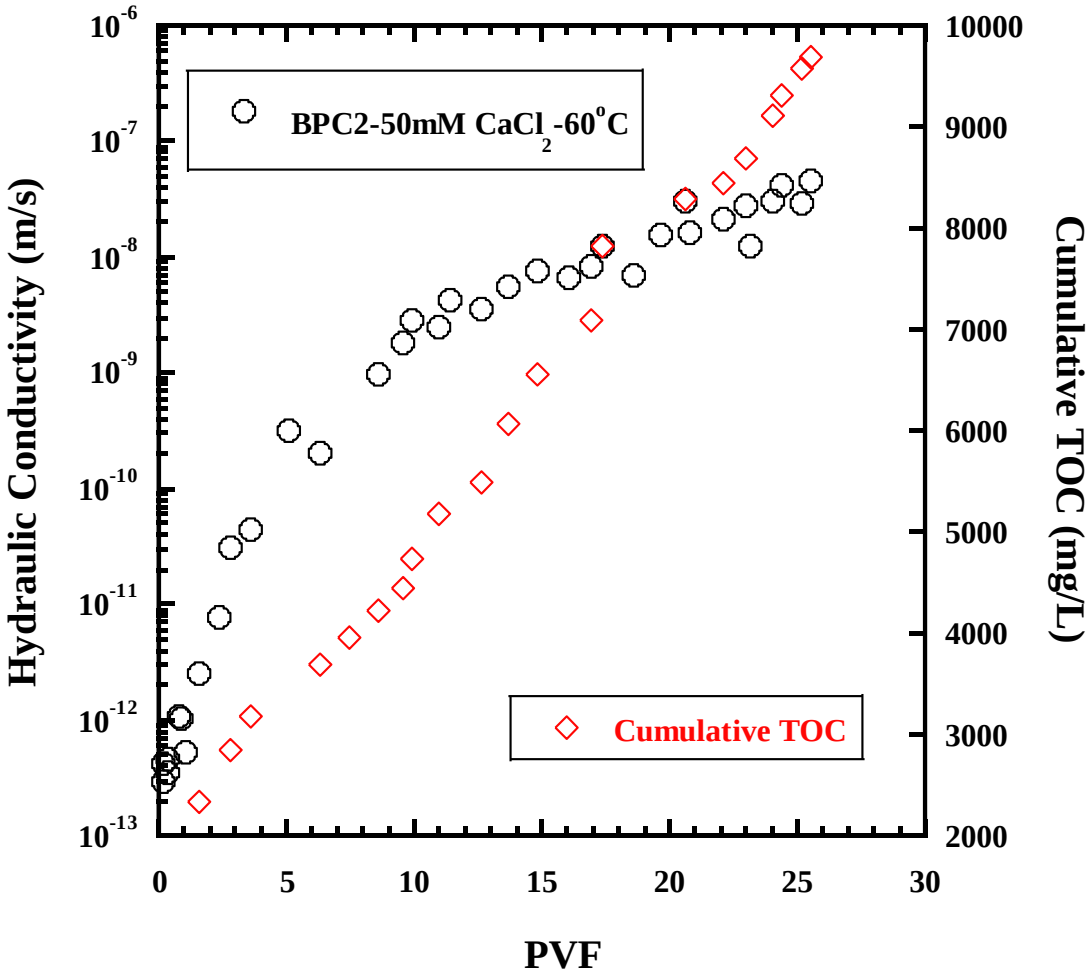

(b)

Figure 3-7. Hydraulic conductivity vs cumulative TOC of BPC2 GCL permeated with 50 mM $CaCl_2$ at (a) 20 °C and (b) at 60 °C.

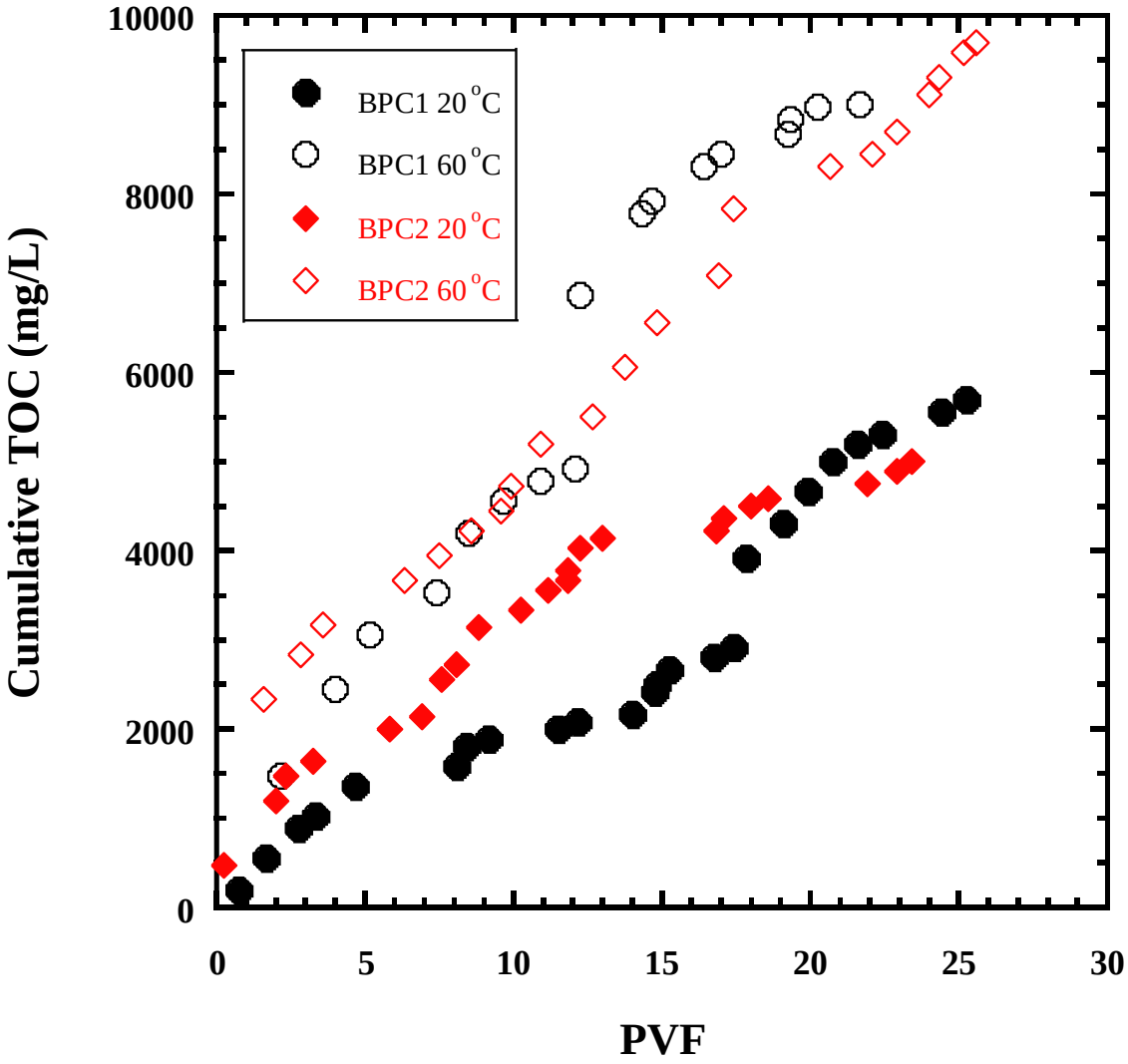

Figure 3-8. Cumulative TOC of BPC1 and BPC2 GCLs at 20, 35, and 60 °C permeated with 50 mM $CaCl_2$

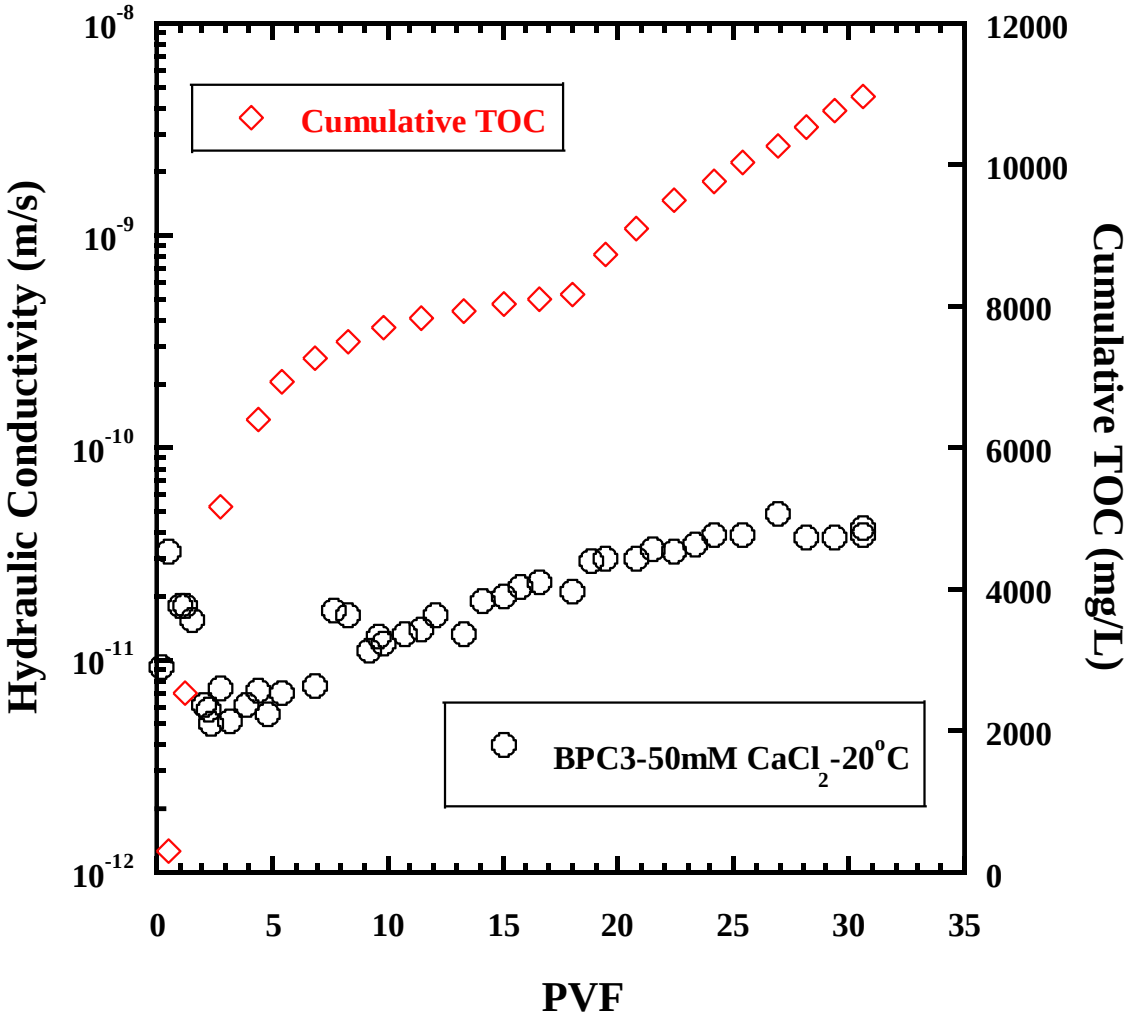
Hydraulic Conductivity (m/s)
Cumulative TOC (mg/L)
PVF
Cumulative TOC
BPC3-50mM CaCl2-20°C
10-8
10-9
10-10
10-11
10-12
12000
10000
8000
6000
4000
2000
0
0
5
10
15
20
25
30
35

(a)

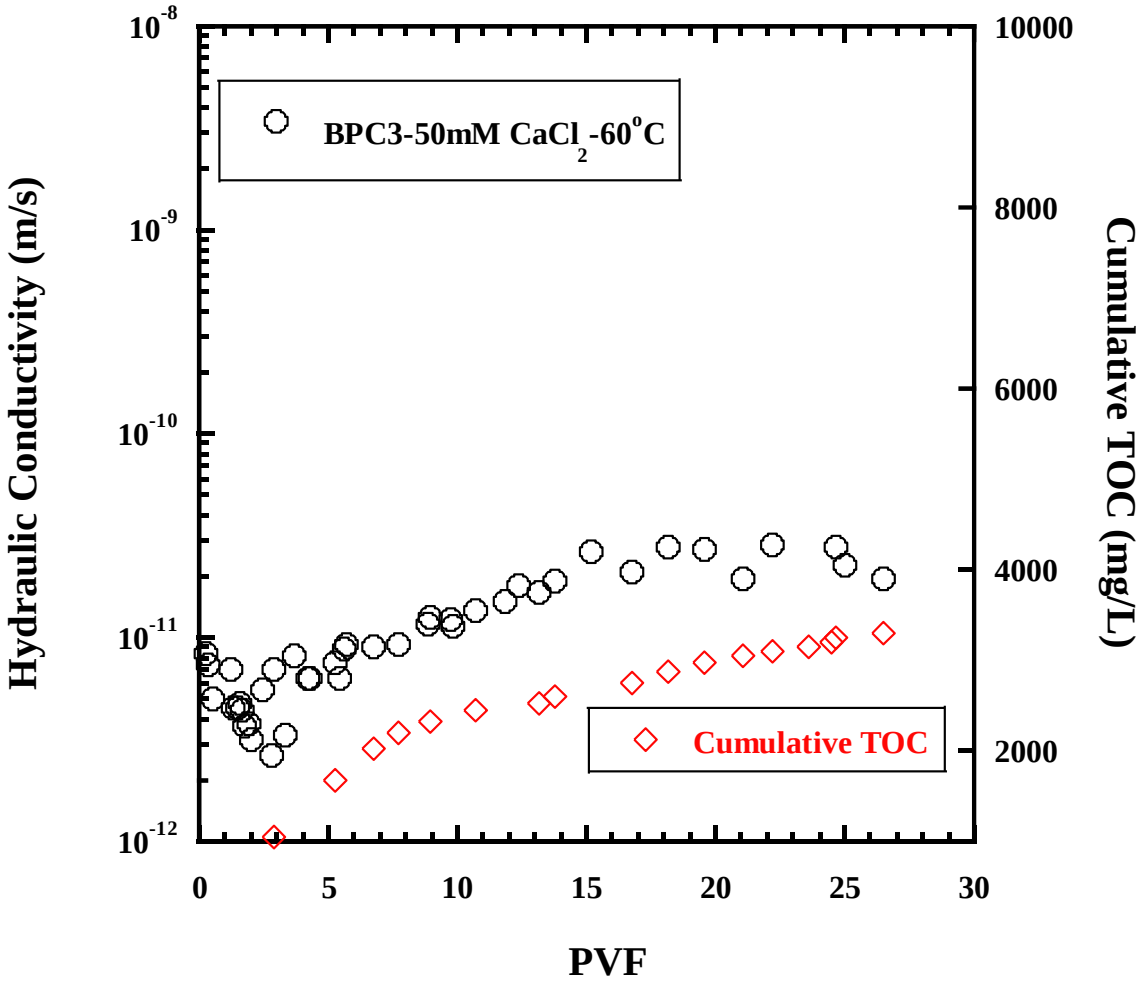

(b)

Figure 3-9. Hydraulic conductivity vs cumulative TOC of BPC3 permeated with 50 mM $CaCl_2$ at (a) 20 °C and (b) at 60 °C

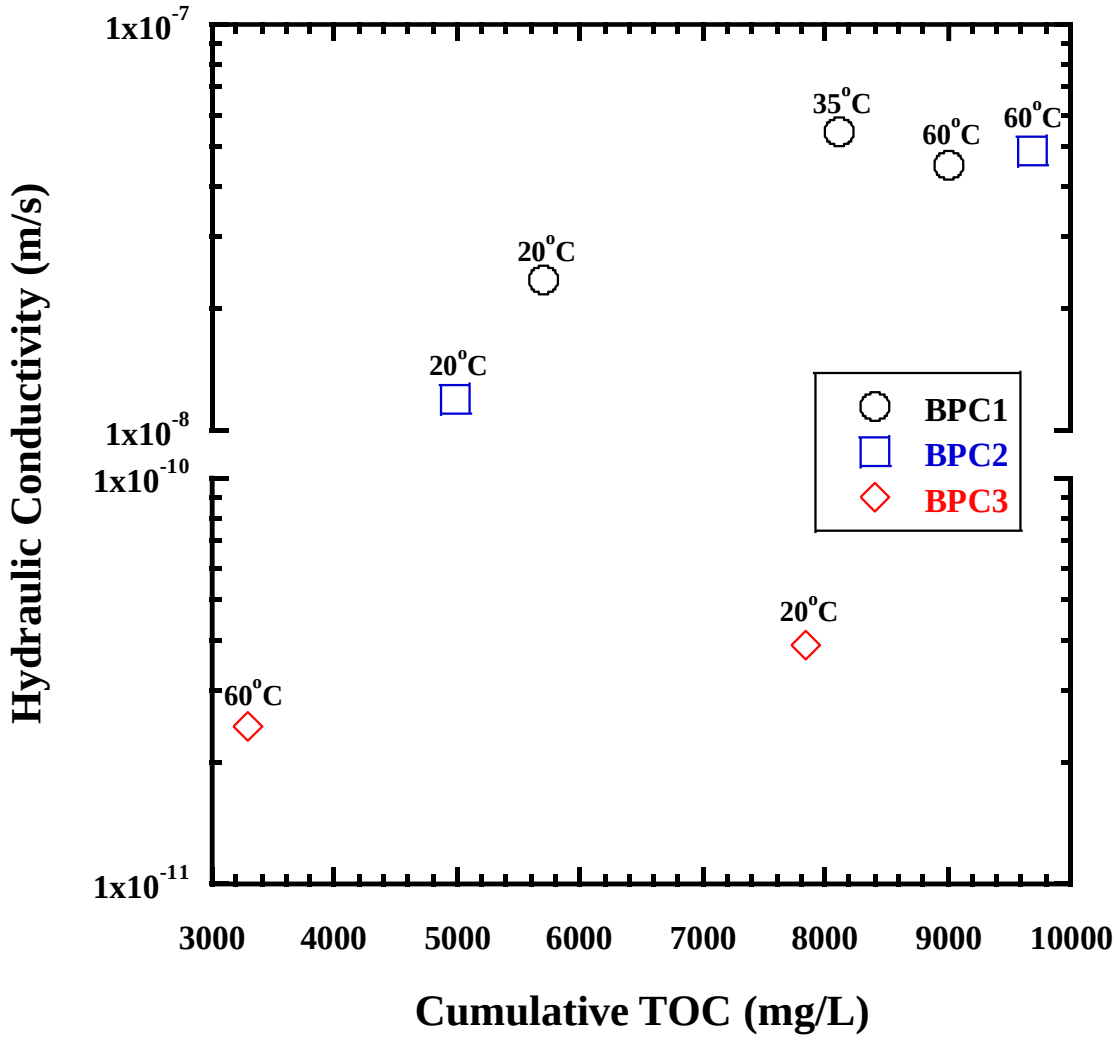

Figure 3-10. Hydraulic conductivities vs cumulative TOC of BPC1, BPC2, BPC3 permeated with 50 mM $CaCl_2$.

Summary and conclusions

Hydraulic conductivity and index tests were performed on three commercially available bentonite polymer composite (BPC) geosynthetic clay liners (GCLs) containing different dry blended polymer loadings at different temperature (e.g., 20, 35, and 60 ^{o}C). The hydraulic conductivity tests and index tests were performed using DI water, 20 mM $CaCl_2$, and 50 mM $CaCl_2$ to represent dilute and moderately aggressive leachates. Swell index and viscosity were conducted to evaluate the property change of BPC at different temperatures. Total organic carbon (TOC) analysis was conducted to evaluate the polymer elution processes during permeation. Tests were also conducted with sodium-bentonite (NaB) GCL as controls. The following conclusions may be drawn based on findings from this study:

- Swell index tests of NaB resulted in a decreasing trend of swell index as temperatures were increased. This phenomenon shows the response of DDL of NaB decreasing in thickness as temperatures were increased and resulted in a slight reduction in swell index. The results for each of the BPC GCLs showed an increasing trend in swell index as temperatures were increased. This increase in swell index as temperatures were increased can be attributed to the polymer content within the BPC virgin soil. This was because all of the BPC GCLs increase in swell index as opposed to NaB which had decreased in swell index as temperatures increased. This supports existing literature that have observed, from experimentation, polymer hydrogels to increase in swell ratio as temperatures were

increased (Owens et al. 2007, Felix et al. 2010, Saeed 2013, Slaughter et al. 2015, Jayaramadu et al. 2019).

- The NaB slurries in each permeant showed to be more viscous than their respective pure permeant solutions, thus noting that NaB soil adds frictional resistance within the leachate to behave as a more viscous sample. Additionally, each of the BPC slurries in each permeant solution also resulted in more viscous sample when compared to NaB slurries in each respective permeant solution. However, at 35 and 60 ^{o}C elevated temperatures, the viscosity of each NaB to saline solution slurries decreased. This can be attributed to a weaker interaction between bentonite particles and water molecules as temperature of permeant solution increases and thus results in a decrease in frictional resistance within the slurry. Furthermore, the decrease in viscosity of each of the BPC solid to liquid slurries can be attributed to a decrease in binding properties of polymer to the bentonite soil.
- Hydraulic conductivity of NaB permeated with DI water performed higher at room temperature and slightly lower at elevated temperatures. However, because of the very large swell capacity of NaB in DI water, the hydraulic conductivity generally results very low ($<10^{-10}$ m/s), and effects of temperature may not affect the overall hydraulic conductivity results. Hydraulic conductivity of each of the GCLs permeated with DI water showed to be less than 10^{-10} (m/s) for all temperatures thus determining that the effect of temperatures were very minimal. BPC1 and BPC2 was observed to show the same trend as NaB in which a small in which the DI water hydraulic conductivity was observed to be higher at room temperature and

slightly lower at elevated temperatures. For the crosslinked BPC3 GCL, a very small increase in hydraulic conductivity was observed.

- Hydraulic conductivity of NaB permeated with 50 mM $CaCl_2$ at 60 ^oC resulted in a hydraulic conductivity approximately two times larger when compared to hydraulic conductivity of NaB with same permeant at room temperature. This increase in hydraulic conductivity supports what was observed in the results for the swell index of NaB when temperatures increased. As temperatures were increased, NaB DDL will decrease and result in a decrease in swell index and thus will result in an increase in hydraulic conductivity.
- Hydraulic conductivity of the linear BPC2 GCL did result in a slightly lower hydraulic conductivity compared to the BPC1 GCL for each respective saline solution and temperature, showing the benefit of an increased amount of polymer content within a GCL. BPC1 and BPC2 GCLs permeated by saline solutions, initially resulted in a very low hydraulic conductivity compared to hydraulic conductivity at room temperature. This decrease in hydraulic conductivity, at low PVF, of the BPC1 and BPC2 GCLs was attributed to the increase in swelling as temperatures were increased. Furthermore, the increased temperatures resulted in an increase in swelling capacity of the polymer hydrogels that effectively decreased hydraulic conductivity initially. However, this decrease in hydraulic conductivity does not last and both linear GCLs were seen to have an increasing trend as more permeant permeated through the GCLs. Final hydraulic conductivity for BPC1 GCL at room temperature was approximately two times lower than the hydraulic

conductivity results at 60 °C. Additionally, the final hydraulic conductivity for BPC2 GCL at room temperature was approximately three times lower than the hydraulic conductivity results at 60 °C.

- Hydraulic conductivity of crosslinked BPC3 to saline solution resulted in the lowest hydraulic conductivity amongst the BPC GCLs. However, it must also be noted that BPC3 has the highest polymer loading content compared to the other BPC GCLs. due to the highest content in polymer loading. Hydraulic conductivity of BPC3 showed opposite trends as what was observed in the linear GCLs. As temperatures were increased, the final hydraulic conductivity was seen to decrease. Furthermore, the hydraulic conductivity of the BPC3 GCL at 20, 35 and 60 °C each showed the same trends noting that the effect elevated temperatures did not affect the crosslink GCL in the same manner as the linear BPC GCLs. Final hydraulic conductivity for BPC3 GCL at room temperature was 1.5 times higher than the hydraulic conductivity results at 60 °C
- TOC measurements resulted in different trends depending on polymer structure within the BPC GCL. Polymer elution for the linear BPC1 and BPC2 GCLs both resulted in increased rates of polymer elution at 60 °C compared to 20 °C. This result can be attributed to the decrease in viscosity of solid to liquid slurries as temperatures were increased that may potentially be due to a reduction in binding properties of polymers to bentonite particles. The increased rates of polymer elution resulted in a hydraulic conductivity that would increase as more polymer eluted for the linear GCLs. However, the crosslinked BPC3 GCL showed opposite trends of

polymer elution. At 60 ^{o}C temperatures, rates of polymer elution decreased because of the physical nature of the crosslink hydrogels. As mentioned previously, the swelling of polymers increased as temperatures were increased. However, the crosslink hydrogel structures act as physical granules that cannot pass through intergranular pore spaces, as opposed to the linear polymers that are liquid soluable. Due to the physical nature of the crosslink hydrogels, polymer hydrogels could potentially be trapped in intergranular spaces as the hydrogel increased in size from an increase in temperatures induced. Thus concluding, that at elevated temperatures, crosslink hydrogels elute at a reduced rate and will then result in lower hydraulic conductivity compared to hydraulic conductivity at room temperature.

Future Research

Accurately assessing the effect of temperature on hydraulic conductivity of GCLs comes with many challenges. BPC GCLs were investigated with moderate strength saline solutions, however industrial waste and hazardous waste landfills will contain more aggressive leachates that can affect hydraulic conductivity of GCLs at elevated temperatures differently than dilute and moderately aggressive solutions. The effect of elevated temperatures can also be investigated with respect to change in pressure of a BPC GCL during heating process and how that would affect polymer elution rates and hydraulic conductivity as a result.

REFERENCES

Ahmed, & Saeed, M. (2013). Temperature Effect on Swelling Properties of Commercial Polyacrylic Acid Hydrogel Beads. Undefined. /paper/Temperature-Effect-on-Swelling-Properties-of-Acid-Ahmed-Saeed/c6acd14a8ed08599128dd472d3c43a9a7cdd140b

ASTM. (2006b). Standard Test Method for swell index of clay mineral component of geosynthetic clay liners. ASTM D 5890-06.

ASTM. (2020a). Standard Test Method for Evaluation of Hydraulic Properties of Geosynthetic Clay Liners Permeated with Potentially Incompatible Aqueous. ASTM D 6766-20a.

ASTM. (2019). Standard Test Method for Fluid Loss of Clay Component of Geosynthetic Clay. ASTM D5891/D5891M-19.

Cho, W. J., Lee, J. O., & Chun, K. S. (1999). The temperature effects on hydraulic conductivity of compacted bentonite. Applied Clay Science, 14(1), 47–58. https://doi.org/10.1016/S0169-1317(98)00047-7

Cho, W., Lee, J., & Chun, K. (1997). Influence of Temperature on Hydraulic Conductivity in Compacted Bentonite. MRS Proceedings, 506, 305. doi:10.1557/PROC-506-305

Gandhi, G., Babu, G., & L G. (2016). Evaluation of engineered barrier system for hazardous waste disposal—A case study. Japanese Geotechnical Society Special Publication, 2, 54–61. https://doi.org/10.3208/jgssp.KL-5

Gao, H., & Shao, M. (2015). Effects of temperature changes on soil hydraulic properties. Soil and Tillage Research, 153, 145–154. https://doi.org/10.1016/j.still.2015.05.003

Geng Weijuan, Likos William J., & Benson Craig H. (n.d.). Viscosity of Polymer-Modified Bentonite as a Hydraulic Performance Index. Geo-Chicago 2016, 498–507. https://doi.org/10.1061/9780784480144.049

Ishimori, H., & Katsumi, T. (2012). Temperature effects on the swelling capacity and barrier performance of geosynthetic clay liners permeated with sodium chloride solutions. Geotextiles and Geomembranes, 33, 25–33. https://doi.org/10.1016/j.geotexmem.2012.02.005

Jayaramudu, T., Ko, H.-U., Kim, H. C., Kim, J. W., & Kim, J. (2019). Swelling Behavior of Polyacrylamide-Cellulose Nanocrystal Hydrogels: Swelling Kinetics, Temperature, and pH Effects. Materials (Basel, Switzerland), 12(13). https://doi.org/10.3390/ma12132080

Jo, H. Y., Katsumi, T., Benson, C. H., & Edil, T. B. (2001). Hydraulic Conductivity and Swelling of Nonprehydrated GCLs Permeated with Single-Species Salt Solutions. Journal of Geotechnical and Geoenvironmental Engineering, 127(7), 557–567. https://doi.org/10.1061/(ASCE)1090-0241(2001)127:7(557)

Jo, H. Y., Benson, C. H., Shackelford, C. D., Lee, J. M., & Edil, T. B. (2005). Long-term hydraulic conductivity of a geosynthetic clay liner permeated with inorganic salt solutions. Journal of Geotechnical and Geoenvironmental Engineering, 131(4), 405-417.

Katsumi, T., Ishimori, H., Onikata, M., & Fukagawa, R. (2008). Long-term barrier performance of modified bentonite materials against sodium and calcium permeant solutions. Geotextiles and Geomembranes, 26(1), 14–30. https://doi.org/10.1016/j.geotexmem.2007.04.003

Koerner, G. R., & Koerner, R. M. (2012). In-Situ Temperature Monitoring of Geomembranes. 1–6. https://doi.org/10.1061/40782(161)48

Kolstad, D. C., Benson, C. H., & Edil, T. B. (2004). Hydraulic Conductivity and Swell of Nonprehydrated Geosynthetic Clay Liners Permeated with Multispecies Inorganic Solutions. Journal of Geotechnical and Geoenvironmental Engineering, 130(12), 1236–1249. https://doi.org/10.1061/(ASCE)1090-0241(2004)130:12(1236)

Mitchell, J. (1993). Fundamentals of soil behavior (2nd ed.). Wiley.

Owens, D. E., Jian, Y., Fang, J. E., Slaughter, B. V., Chen, Y.-H., & Peppas, N. A. (2007). Thermally Responsive Swelling Properties of Polyacrylamide/Poly(acrylic acid) Interpenetrating Polymer Network Nanoparticles. Macromolecules, 40(20), 7306–7310. https://doi.org/10.1021/ma071089x

Ozhan, H. O. (2018). Hydraulic capability of polymer-treated GCLs in saline solutions at elevated temperatures. Applied Clay Science, 161, 364–373. https://doi.org/10.1016/j.clay.2018.05.007

Patel, N. H. (2005). Hydraulic conductivity of geosynthetic clay liners permeated at elevated temperatures [M.S., Michigan State University]. https://search.proquest.com/docview/305476762/abstract/608F9A1D9B044F15PQ/1

Petrov, R. J., & Rowe, R. K. (1997). Geosynthetic clay liner (GCL)- chemical compatibility by hydraulic conductivity testing and factors impacting its performance. Canadian Geotechnical Journal, 34(6), 863–885.

Prongmanee, N., & Chai, J.-C. (2019). Performance of Geosynthetic Clay Liner with Polymerized Bentonite in Highly Acidic or Alkaline Solutions. International Journal of

Geosynthetics and Ground Engineering, 5(3), 26. https://doi.org/10.1007/s40891-019-0177-7

Razakamanantsoa, A. R., Barast, G., & Djeran-maigre, I. (2012). Hydraulic performance of activated calcium bentonite treated by polyionic charged polymer. Applied Clay Science, 59–60, 103–114. https://doi.org/10.1016/j.clay.2012.01.022

Rodríguez-Félix, D. E., Castillo-Ortega, M. M., Real-Félix, D., Romero-García, J., Ledezma-Pérez, A. S., & Rodríguez-Félix, F. (2011). Synthesis and swelling properties of pH- and temperature-sensitive interpenetrating polymer networks composed of polyacrylamide and poly(γ-glutamic acid). Journal of Applied Polymer Science, 119(6), 3531–3537. https://doi.org/10.1002/app.33006

Rowe, R. (1998, March 1). Geosynthetics and the minimization of contaminant migration through barrier systems beneath solid waste.

Sari, K., & Chai, J. (2013). Self healing capacity of geosynthetic clay liners and influencing factors. Geotextiles and Geomembranes, 41, 64–71. https://doi.org/10.1016/j.geotexmem.2013.08.006

Scalia, J., Benson, C. H., Bohnhoff, G. L., Edil, T. B., & Shackelford, C. D. (2014). Long-Term Hydraulic Conductivity of a Bentonite-Polymer Composite Permeated with Aggressive Inorganic Solutions. Journal of Geotechnical and Geoenvironmental Engineering, 140(3), 04013025. https://doi.org/10.1061/(ASCE)GT.1943-5606.0001040

Shackelford, C. (1994). Waste-Soil Interactions that Alter Hydraulic Conductivity. In D. Daniel & S. Trautwein (Eds.), Hydraulic Conductivity and Waste Contaminant Transport in Soil (pp. 111-111–158). ASTM International. https://doi.org/10.1520/STP23887S

Shackelford, C. D., Benson, C. H., Katsumi, T., Edil, T. B., & Lin, L. (2000). Evaluating the hydraulic conductivity of GCLs permeated with non-standard liquids. Geotextiles and Geomembranes, 18(2), 133–161. https://doi.org/10.1016/S0266-1144(99)00024-2

Slaughter, B. V., Blanchard, A. T., Maass, K. F., & Peppas, N. A. (2015). Dynamic swelling behavior of interpenetrating polymer networks in response to temperature and pH. Journal of Applied Polymer Science, 132(24). https://doi.org/10.1002/app.42076

Tian, K., Benson, C. H., & Likos, W. J. (2016). Hydraulic Conductivity of Geosynthetic Clay Liners to Low-Level Radioactive Waste Leachate. Journal of Geotechnical and Geoenvironmental Engineering, 142(8), 04016037. https://doi.org/10.1061/(ASCE)GT.1943-5606.0001495

Tian, K., Likos, W. J., & Benson, C. H. (2019). Polymer Elution and Hydraulic Conductivity of Bentonite–Polymer Composite Geosynthetic Clay Liners. Journal of Geotechnical and Geoenvironmental Engineering, 145(10), 04019071. https://doi.org/10.1061/(ASCE)GT.1943-5606.0002097

Touze-Foltz, N., Xie, H., & Stoltz, G. (2018). Performance Issues of Barrier Systems for Landfills. Proceedings of the 8th International Congress on Environmental Geotechnics Volume 1, 81–98. https://doi.org/10.1007/978-981-13-2221-1_4

Vryzas, Z., Kelessidis, V. C., Nalbantian, L., Zaspalis, V., Gerogiorgis, D. I., & Wubulikasimu, Y. (2017). Effect of temperature on the rheological properties of neat aqueous Wyoming sodium bentonite dispersions. Applied Clay Science, 136, 26–36. https://doi.org/10.1016/j.clay.2016.11.007

Wang, S., Zhu, W., Qian, X., Xu, H., & Fan, X. (2017). Temperature effects on non-Darcy flow of compacted clay. Applied Clay Science, C(135), 521–525. https://doi.org/10.1016/j.clay.2016.09.025

Wang, X. and Benson, C. (1999). Hydraulic Conductivity Testing of Geosynthetic Clay Liners (GCLs) Using the Constant Volume Method. Geotechnical Testing Journal, 22 (4), 277-283. Retrieved from https://doi.org/10.1520/GTJ11239J

Ye, W. M., Wan, M., Chen, B., Chen, Y. G., Cui, Y. J., & Wang, J. (2013). Temperature effects on the swelling pressure and saturated hydraulic conductivity of the compacted GMZ01 bentonite. Environmental Earth Sciences, 68(1), 281–288. http://dx.doi.org/10.1007/s12665-012-1738-4

Yeşiller, N., Hanson, J. L., & Liu, W.-L. (2005). Heat Generation in Municipal Solid Waste Landfills. Journal of Geotechnical and Geoenvironmental Engineering, 131(11), 1330–1344. https://doi.org/10.1061/(ASCE)1090-0241(2005)131:11(1330)

Yeung, A. T. (1992). Diffuse Double-Layer Eqautions in SI Units. Journal of Geotechnical Engineering, 118(12), 2000–2005. https://doi.org/10.1061/(ASCE)0733-9410(1992)118:12(2000)

Zainab, B. (2020). *Hydraulic Conductivity of Bentonite-Polymer (B-P) Geosynthetic Clay Liners (GCLs) to Aggressive Coal Combustion Product (CCP) Leachates* [Thesis]. http://mars.gmu.edu/handle/1920/11684

BIOGRAPHY

Andres Javier Cruz graduated from Thomas Edison High School, Virginia, United States, in 2014. He received his Bachelors in Civil Engineering from George Mason University in 2019. He decided to continue research work with a geo-environmental background at the same university to do his Thesis study and complete Masters of Science in Civil Engineering at George Mason University. He finished his graduate studies in 2021.